

L-665  
NATIONAL ADVISORY COMMITTEE FOR AERONAUTICS

# WARTIME REPORT

ORIGINALLY ISSUED

May 1944 as

Advance Confidential Report L4E13

ANALYSIS OF AVAILABLE DATA ON CONTROL SURFACES

HAVING PLAIN-OVERHANG AND FRISE BALANCES

By Paul E. Purser and Thomas A. Toll

Langley Memorial Aeronautical Laboratory  
Langley Field, Va.

LIBRARY  
NATIONAL ADVISORY COMMITTEE FOR AERONAUTICS

CASCOM  
L4E13

# NACA

WASHINGTON

NACA WARTIME REPORTS are reprints of papers originally issued to provide rapid distribution of advance research results to an authorized group requiring them for the war effort. They were previously held under a security status but are now unclassified. Some of these reports were not technically edited. All have been reproduced without change in order to expedite general distribution.



NATIONAL ADVISORY COMMITTEE FOR AERONAUTICS

---

ADVANCE CONFIDENTIAL REPORT

---

ANALYSIS OF AVAILABLE DATA ON CONTROL SURFACES

HAVING PLAIN-OVERHANG AND FRISE BALANCES

By Paul E. Purser and Thomas A. Toll

SUMMARY

The available data on control surfaces having plain-overhang and Frise balances have been analyzed and some empirical relations that will facilitate the prediction of the characteristics of balanced control surfaces from the geometric constants have been determined. The analysis presented has been limited to the effects of overhang, nose shape, gap, and Mach number. Although the relations given are not considered sufficiently reliable to allow satisfactory prediction of airplane stick forces without the aid of wind-tunnel tests of a scale model, they are considered applicable to the preliminary design of control-surface balances and to modifications of balances already in use.

The effects of balance variations in changing the slope of the curve of hinge-moment coefficient plotted against control-surface deflection and in changing the lift effectiveness of the control surface are correlated for low Mach numbers by a balance factor that accounts for the length and shape of overhang. No such factor was obtained that would adequately account for all of the variables affecting the slope of the curve of hinge-moment coefficient plotted against angle of attack or the deflection range over which the balance is effective in reducing the slope of the hinge-moment curve. The effects of gap and Mach number are presented for a few representative models. Some representative pressure-distribution diagrams are presented for controls with plain-overhang and Frise balances.

INTRODUCTION

The demands for more maneuverability and smaller control forces for high-speed combat aircraft and the

general increase in the size and speed of all types of airplane have resulted in a considerable amount of research on means for balancing control surfaces. The results of a great part of the control-surface research have recently been collected in two papers: one generally applicable to ailerons (reference 1), and the other generally applicable to tail surfaces (reference 2). The data contained in the two collections and in other papers are being analyzed, correlated, and summarized at LMAL. The results of these studies are being published separately as they are completed. Reference 3 contains information on internally balanced controls, reference 4 contains information on controls with beveled trailing edges and similar contour modifications, and reference 5 contains data on horn-balanced controls.

The present paper deals with control surfaces having plain-overhang and Frise balances. The effects of overhang, nose shape, gap, and Mach number have been studied. The Frise balance is considered only as a special type of overhang balance, and certain characteristics generally associated only with Frise balances - such as the effects of bulges, vent gaps, slot shapes, and the vertical locations of the hinge axes - have not been considered. Such effects may sometimes be appreciable, but they cannot be properly evaluated from the existing data.

#### SYMBOLS

The coefficients, parameters, factors, and symbols used in correlating and presenting the data are:

$C_L$	lift coefficient
$c_l$	section lift coefficient
$C_{L1}$	average lift coefficient over control-surface span for airfoil with plain sealed control surface
$c_{l1}$	section lift coefficient for airfoil with plain sealed control surface
$C_h$	hinge-moment coefficient

$c_h$	section hinge-moment coefficient
$P$	pressure coefficient $\left(\frac{p - p_o}{q}\right)$
$p$	local static pressure
$p_o$	static pressure in undisturbed airstream
$q$	dynamic pressure of undisturbed airstream $\left(\frac{1}{2}\rho v^2\right)$
$\alpha$	angle of attack, degrees
$\delta_f$	control-surface deflection relative to airfoil, degrees
$\delta_{cr}$	critical control-surface deflection; that is, deflection at which plain-overhang or Frise balance is no longer effective in reducing slope of hinge-moment curve (approximately the deflection at which maximum lift is obtained for a given angle of attack)
$c$	airfoil chord
$\bar{c}$	root-mean-square airfoil chord over span of control surface
$c_f$	control-surface chord back of hinge line
$\bar{c}_f$	root-mean-square control-surface chord
$c_b$	balance chord, distance from hinge line to leading edge of plain-overhang or Frise balance
$\bar{c}_b$	root-mean-square balance chord
$c_b'$	contour balance chord, distance from hinge line to point of tangency of balance leading-edge arc and airfoil contour
$\bar{c}_b'$	root-mean-square contour balance chord
$t$	thickness of airfoil section at hinge line
$\bar{t}$	root-mean-square of airfoil section thickness at hinge line

$b_f$	span of control surface
$b_o$	span of plain-overhang or Frise balance
$A$	aspect ratio
$\lambda$	ratio of tip chord to root chord
$M$	Mach number; with subscripts, area moment of the balance profile about hinge axis
$R$	Reynolds number; with subscripts, balance nose radius
$l$	chord-wise location of minimum-pressure point for low-drag airfoils measured in airfoil chords from leading edge (one-tenth of second digit in low-drag airfoil designation, reference 6)

$F_1$  overhang factor

$F_2, F_2'$  nose-shape factors

$K_1$  balance factor ( $F_1 F_2'$ )

Subscripts

O, A, B, C, D, E, F, G, denote overhang-nose type (table I)

and

$$C_{L\alpha} = \left( \frac{\partial C_L}{\partial \alpha} \right)_{\delta_f}$$

$$C_{l\alpha} = \left( \frac{\partial C_l}{\partial \alpha} \right)_{\delta_f}$$

$$C_{L1\alpha} = \left( \frac{\partial C_{L1}}{\partial \alpha} \right)_{\delta_f}$$

$$C_{l1\alpha} = \left( \frac{\partial C_{l1}}{\partial \alpha} \right)_{\delta_f}$$

$$c_{l\delta} = \left( \frac{\partial c_l}{\partial \delta_f} \right)_\alpha$$

$$c_{l1\delta} = \left( \frac{\partial c_{l1}}{\partial \delta_f} \right)_\alpha$$

$$C_{h\alpha} = \left( \frac{\partial C_h}{\partial \alpha} \right)_{\delta_f}$$

$$C_{h\alpha} = \left( \frac{\partial C_h}{\partial \alpha} \right)_{\delta_f}$$

$$C_{h\delta} = \left( \frac{\partial C_h}{\partial \delta_f} \right)_\alpha$$

$$C_{h\delta} = \left( \frac{\partial C_h}{\partial \delta_f} \right)_\alpha$$

k lift-effectiveness parameter  $\left( \frac{c_{l\delta}}{c_{l\alpha}} \right)$

$k_o$  lift-effectiveness parameter for plain scaled flaps  $\left( \frac{c_{l1\delta}}{c_{l1c}} \right)$

The subscripts outside the parentheses indicate the factors held constant during measurement of the parameters.

$\Delta C_{h\alpha}$   
 $\Delta C_{h\alpha}$   
 $\Delta C_{h\delta}$   
 $\Delta C_{h\delta}$

increments of slopes of hinge-moment curves due to overhang type of balance for test conditions using data for plain unbalanced control surface with same gap condition as a base

## AVAILABLE DATA

The data used in the summary were obtained from the results of model tests presented in references 7 to 24 and also from various unpublished test results. Some of the more pertinent information regarding the geometric characteristics of the models and the test conditions are summarized in table II.

Although an appreciable amount of data from tests of two-dimensional control surfaces and finite-span ailerons were available, the amount of data obtained for finite-span tail surfaces was not considered adequate for a reliable correlation.

The values of the slopes of the hinge-moment curves used in the analysis are the slopes for small control deflections at an angle of attack of  $0^\circ$ .

## CORRELATION METHODS

The present paper is concerned with the generalization of the effects of plain-overhang and Frise balances in providing aerodynamic balance for flap-type control surfaces. Empirical factors and design charts were desired in order that approximate relations could be established between the geometric constants of overhang balances and the effects of overhang balances on the hinge-moment slopes. A preliminary study of the problem, indicated that the slope increments  $\Delta C_{h\delta}$  and  $\Delta C_{h\alpha}$  (or  $\Delta c_{h\delta}$  and  $\Delta c_{h\alpha}$ ) due to the overhang were more suitable for correlation than the total values of the slopes.

The aerodynamic balancing effect of an overhang balance is considered to be a maximum when the contour of the balance conforms to the contour of the airfoil for the entire length of the overhang. Rounding or tapering the nose causes a reduction in the effect of the balance. In the present analysis, the effects of overhang length and nose shape were evaluated independently by means of various cross plots of the available data. The effects of variations in the nose shape were found to depend on the overhang length; therefore, a measure



of the net balancing effect of plain-overhang or Frise balances was obtained as a product rather than as a difference of two empirical factors. The two factors are  $F_1$ , which is related to the length of overhang, and  $F_2'$ , which is related to the sectional shape of the balance nose. Thus

$$K_1 = F_1 F_2'$$

where

$$F_1 = \left[ \left( \frac{\bar{c}_b}{\bar{c}_f} \right)^2 - \left( \frac{t/2}{\bar{c}_f} \right)^2 \right] \frac{b_b}{b_f}$$

and the expression for  $F_2'$  is given in table I for various general types of nose shape. As may be seen from table I, the expression for  $F_2'$  is, in general, the product of an area-moment ratio and a basic nose-shape factor that specifies the relative location of the point of tangency of a circular-arc nose and the airfoil contour. This basic nose-shape factor  $F_2$  is defined as

$$F_2 = 1 - \sqrt{1 - \left( \frac{1 + \frac{\bar{c}_b'}{\bar{c}_f}}{1 + \frac{\bar{c}_b}{\bar{c}_f}} \right)^2}$$

It should be noted that for any overhang having a nose formed by circular arcs (nose types C, A, B, D, and G of table I)

$$F_2' = F_2$$

and therefore

$$K_1 = F_1 F_2$$

If the nose shape is elliptical (type C, table I) or sharp (type E or F, table I) the factor  $F_2'$  is obtained by multiplying a nominal value of  $F_2$  by an area-moment factor. For an elliptical nose (type C) the nominal value of  $F_2$  is the value that would be obtained for a flap having the same overhang as the given flap but with a nose shape of type B. The appropriate area-moment factor is given in table I where  $M_0$ ,  $M_B$ , and  $M_C$  are the area moments about the hinge axis of the balance profiles having nose types denoted by the subscript letters. A similar method is used for the sharp-nose balances (E and F). In these cases, the nominal value of  $F_2$  is obtained for a circular-arc nose (type D) having a radius  $R_D$  such that the arc becomes tangent to the airfoil contour at a point defined by the intersection of the airfoil contour and an extension of the straight line forming the forward portion of the balance nose. The exponents of the area-moment factors were determined empirically.

Graphical solutions of the expressions for the overhang factor  $F_1$  (for overhangs having spans equal to the control-surface span) and the basic nose-shape factor  $F_2$  are presented in figure 1. The value of  $F_1$  for balances which do not extend over the entire span of the control surface (as for conventional rudders) is obtained by multiplying the value of  $F_1$  obtained from figure 1 by the ratio of balance span to control-surface span. The use of this figure should allow a rapid determination of  $F_1$  and  $F_2$ , provided the geometric constants  $\bar{c}_b$ ,  $\bar{c}_b'$ ,  $\bar{t}$ , and  $\bar{c}_f$  are known.

The analysis of the available data on control surfaces with beveled trailing edges (reference 4) indicated that the effects of plan form of the wing or tail surface could be accounted for reasonably well by assuming that both the lift-curve slope and the increments of hinge-moment slopes due to aerodynamic balance are affected by plan-form changes in the same manner. The same assumption has been made in the present correlation of the variation of hinge moments with control deflection.

In the original reports of the partial-span model tests (models X, XVIII, and XIX of table II) plan-form corrections were not applied to the hinge-moment data

but were applied to the other aerodynamic characteristics. The lift characteristics used for these three models in this correlation are those corresponding to the actual portion of the model tested and are not the same as previously presented lift characteristics.

## RESULTS

### Hinge-Moment Parameters

The effects of overhang balances on the variation of hinge-moment coefficient with control deflection are shown in figure 2 as curves of  $\Delta C_{h\delta}/C_{L1\alpha}$  or  $\Delta c_{h\delta}/c_{l1\alpha}$  plotted against the balance factor  $K_1$ . The parameter  $C_{L1\alpha}$  is the average value of the lift-curve slope over the span of the control surface and is generally somewhat different from the lift-curve slope of the entire wing. A method of estimating the value of  $C_{L1\alpha}$  for ailerons on wings of various plan forms is given in reference 4. For conventional tail surfaces,  $C_{L1\alpha}$  generally may be assumed equal to the lift-curve slope of the entire surface. As shown by figure 2, the variation of the parameter  $\Delta C_{h\delta}/C_{L1\alpha}$  with  $K_1$  for finite-span ailerons was the same as the variation of  $\Delta c_{h\delta}/c_{l1\alpha}$  with  $K_1$  for two-dimensional flaps. The relation was somewhat different, however, for finite-span tail surfaces from that for finite-span ailerons or two-dimensional flaps. No attempt has been made to account for the difference, but the assumption that hinge-moment slope increments and the lift-curve slope vary in the same manner with plan form is probably not valid for the very low aspect ratios normally used for tail surfaces. The relation indicated for finite-span tail surfaces is based on test results of relatively few models and cannot therefore be considered as reliable as the relation shown for finite-span ailerons and two-dimensional flaps.

Values of  $\Delta C_{h\delta}/C_{L1\alpha}$  and  $\Delta c_{h\delta}/c_{l1\alpha}$  (for negative deflections only) for ailerons and flaps having Frise balances had essentially the same relation to the balance factor  $K_1$  as did the values for ailerons and flaps having plain-overhang balances. The Frise data are presented in a separate plot, however, in order to show the limits of  $K_1$  covered by the available data.

First-approximation values of  $\bar{c}_b/\bar{c}_f$  required for given values of  $K_1$  may be obtained for nose shapes of types A, B, or D from figure 3. This figure was derived from the ordinates of NACA conventional airfoils as given in reference 25, and values of  $\bar{c}_b/\bar{c}_f$  obtained from this figure may be accepted as the final values for any airfoil of the NACA conventional four-digit or five-digit series. For other airfoils, figure 3 should be used only for determining first-approximation values of  $\bar{c}_b/\bar{c}_f$ . By use of figure 1 and one or two additional approximations the final values may be obtained.

No factor was obtained that would adequately account for all the variables which effect the variation of hinge-moment coefficient with angle of attack. The variations of  $\Delta C_{h\alpha}$  and  $\Delta c_{h\alpha}$  with the overhang factor  $K_1$  are presented in figure 4 for representative models having various nose shapes and open or sealed gaps. As may be seen from figure 4  $\Delta C_{h\alpha}$  or  $\Delta c_{h\alpha}$  increases with overhang, but the increase is less rapid for medium noses (type C) or sharp noses (type F) than for blunt noses (type B). The effect of nose shape is much greater when the gap is open than when the gap is sealed and sealing the gap generally results in a decrease in  $\Delta C_{h\alpha}$  or  $\Delta c_{h\alpha}$  for a given balance. Little consistency in the magnitude of the decrease can be noted from figure 4.

#### Deflection Range

Attempts to correlate  $\delta_{cr}$ , the deflection at which the overhang loses its balancing effect, with the balance factor  $K_1$  gave unsatisfactory results. A somewhat

better correlation was obtained with the function  $\frac{F_2 \sqrt{F_1}}{(1 - \lambda^2)}$

in which the factor  $1 - \lambda^2$  serves to account for the lower values of  $\delta_{cr}$  obtained for low-drag airfoils. The scatter of points in figure 5, which presents the correlation of  $\delta_{cr}$  for  $\alpha = 0^\circ$ , is probably still too great to justify use of the given relation in original design work. The given relation, however, should allow satisfactory estimates of the change in  $\delta_{cr}$  that might be expected to accompany minor modifications to the overhang or nose shape of balances already in use.

### Lift Effectiveness

Several investigations have indicated that the lift effectiveness of a flap is a function of the overhang balance and the gap. Reasonably consistent variations of the effectiveness ratio  $k/k_0$  with the balance factor  $K_1$  were obtained and are presented in figure 6 for several different gaps. The test values plotted are principally for 30-percent-chord flaps (only a few points for 20-percent-chord flaps were available) but the relations shown in figure 6 are believed to apply reasonably well within the limits of chord ratios normally used for control surfaces. The effectiveness parameter  $k$  for a flap having a given gap and balance factor  $K_1$  may be determined by multiplying the value of  $k/k_0$  obtained from figure 6 by the effectiveness parameter  $k_0$  for a plain sealed flap having the same chord ratio  $c_f/c$ . That the effectiveness parameter  $k$  increases with the balance factor  $K_1$  and that the rate of increase is greater for the larger gaps may be seen from figure 6. If the four curves of figure 6 had been plotted from the same base, they would intersect near  $k/k_0 = 1.05$  where  $K_1 = 0.05$ . Thus, for  $K_1$  values greater than 0.05, opening a gap will generally increase  $k$ , and for  $K_1$  values less than 0.05, opening a gap will generally decrease  $k$ . Although the lift effectiveness increases as the amount of balance increases, the uninstalled deflection range decreases (fig. 5). The maximum increment of lift of a highly balanced control surface is generally somewhat less than the maximum increment of lift of the corresponding unbalanced control surface.

### Effect of Gap

The effect of gap on the section hinge-moment parameters and on the critical deflection is given for a few representative two-dimensional models in figure 7. For the conventional airfoils for which results are shown there was a tendency for the values of  $ch_a$  and  $ch_\delta$  to become less negative as the gap was increased. For the low-drag airfoil (model II), however, the values of  $ch_a$  and  $ch_\delta$  became more negative as the gap was increased. The variations noted for the various airfoils are in agreement with the statement in reference 4 that opening a gap increases the tendency of larger trailing-edge angles to make the hinge-moment parameters more positive.

The magnitude of the critical deflection decreased with gap for the two models shown in figure 7. The rate of decrease of  $\delta_{cr}$  was greater for the low-drag airfoil (model II) than for the conventional airfoil (model I).

### Effect of Mach Number and Reynolds Number

The effect of a simultaneous increase in Mach number and Reynolds number on the hinge-moment parameters, the lift-effectiveness parameter, and the critical deflection is shown for three representative models in figure 8. The data are too scarce and the variations too irregular to justify any generalizations except with regard to the critical deflection, which decreased as the Mach number increased for all three cases. The variation of  $\delta_{cr}$  with  $M$  was slightly greater for flaps with sealed gaps than for flaps with open gaps.

The tendency for  $ch_a$  and  $ch_\delta$  to become less negative at the higher Mach numbers as noted for some airfoils is important because it may lead to control-force overbalance at high speed. The available data are too meager, however, to warrant rating the various airfoils and types of overhang on this basis.

### Pressure Distributions

Data on the pressure distributions over control surfaces with plain-overhang and Frise balances are relatively scarce but a few sample diagrams from references 1, 19, and 26 are presented in figures 9 to 13. Additional data may be obtained from references 27 and 28.

The effects of nose radius, gap, and control-surface deflection on the pressures over control surfaces with plain-overhang balances is shown for a two-dimensional model in figure 9 and for a finite-span model in figure 10. Within the unstalled range, decreasing the nose radii had little effect on the pressures back of the hinge but increased the peak pressure at the protruding nose of the balance. Control surfaces with very small nose radii stalled at relatively low deflections. Sealing the gap decreased the positive pressures on the upper surface of the balance for negative deflections but had a negligible effect on the pressures over other portions of the control surface.

The effect of Mach number on the pressure distribution over a control surface with plain-overhang balance is shown in figure 11 for control-surface deflections of  $\pm 10^\circ$ . The increase in peak negative pressure, which usually accompanies an increase in Mach number, is not evident in figure 11. Evidently the adverse pressure gradient back of the balance nose was so great that the control surface stalled at some intermediate Mach number. Pressure surveys over the lower surface at the nose and the upper surface at the hinge line of a Frise aileron on a semispan model of a low-drag wing are shown in figure 12.

The effects of nose radius, vent gap, and modifications to the slot-entry shape are shown in figure 13 for a control surface with a Frise balance. Decreasing the nose radius with this control had effects similar to those noted previously for the plain-overhang control; that is, the peak negative pressures were increased for every case except for the smallest nose radius, with which the nose was stalled at the deflection for which the diagram is shown. Increasing the vent gap or rounding the slot entry slightly reduced the negative pressures over the balance nose for negative deflections and the positive pressures over the balance nose for positive deflections. Rounding the slot entry and

increasing the vent gap increased the flow velocity through the slot, as is evidenced by the more negative pressures over the upper surfaces of the balance and of the control at positive deflections.

#### OPTIMUM BALANCE ARRANGEMENTS

Many factors must be considered in selecting the optimum overhang-balance arrangement for a given control surface. The following is a brief discussion of some of these factors.

A given value of  $\Delta C_{h_0}$  may be obtained by many variations of balance length and nose shape ranging from rather short and blunt balances to longer balances with sharp noses. Although the geometric characteristics may be adjusted over quite a wide range for any given value of  $\Delta C_{h_0}$ , other aerodynamic characteristics will not remain constant and, consequently, must be considered.

The fact that  $\delta_{cr}$  varies approximately as  $F_2' \sqrt{F_1}$ , whereas  $\Delta C_{h_0}$  varies as  $F_2' F_1$ , indicates that a long overhang and a moderate nose shape of type B, C, or D is more satisfactory than a short overhang and a blunt-nose shape of type A.

A factor that is probably quite closely related to  $\delta_{cr}$  is the magnitude of the peak pressures over the balance nose. If  $\Delta C_{h_0}$  is assumed to remain the same, a short blunt-nose balance produces higher peak pressures than a long balance with a moderate nose shape. The high peak pressure associated with the very blunt nose shape increases the possibility that the control surface may become overbalanced at high Mach numbers and probably increases the rate at which Mach number reduces the value of  $\delta_{cr}$ . The high peak pressures increase the possibility that supercritical local velocities will be reached over the nose of the balance. Although little definite information is at present available concerning the effects of shock waves that occur over only a relatively short chordwise portion of the airfoil, such effects are probably not beneficial.



The ease with which static balance may be obtained is important, especially for large airplanes. The long overhangs permit static balance to be obtained by the addition of a minimum of otherwise nonuseful weight.

Other considerations impose limitations on the most desirable length of overhang. A long overhang requires a large part of the fixed structure of the wing or tail surface to be cut away to allow for free movement of the balance. The large breaks in the airfoil surface that result from the use of medium or sharp nose shapes probably increase the drag.

Nose shapes of types C, D, E, or F are likely to give overbalance at high deflections if designed for slight underbalance at low deflections because a large portion of the balancing action of the overhang type of balance is produced by the negative pressure developed at the portion of the nose that protrudes above or below the airfoil contour. For nose types C and D the negative pressure peak moves forward and increases in magnitude as the deflection is increased, thereby resulting in an effective increase in balance. From these considerations it might be mentioned that a shape of type D can be expected to be more satisfactory than a shape of type C, unless the deflection limits allow the most forward point of the nose to protrude outside the airfoil contour. All the pointed nose shapes (types D, E, and F) show a greatly increased balancing effect when the nose protrudes above or below the airfoil contour. It appears that such a condition should be avoided by the use of stops unless the control deflection required would be beyond the critical value and it is desired to use the control in this condition. Control surfaces with blunt-nose overhangs (types A and B) have also shown some tendency toward increased balance at high deflections (references 7 and 19) but the effect is not as great as for the medium- and sharp-nose shapes just discussed.

As pointed out in a previous section the parameter  $\Delta C_{h_0}$  is relatively independent of nose shape for sealed balances and appears to depend principally on the balance chord. The choice of the best combination of nose shape and overhang for a given  $\Delta C_{h_0}$  may therefore be influenced by the value of  $\Delta C_{h_0}$  obtained, the degree of influence depending on the specific application.

The choice of an open or a sealed gap for use with the overhang will be influenced by the fact that nose shape has more effect on  $C_{h_a}$  with the gap open than with the gap sealed. For balances having values of  $K_1$  greater than about 0.05 the use of an open gap generally increases the lift-effectiveness parameter  $k$  of the control surface. Part of the gain in  $k$ , however, is obtained at the expense of a loss in  $c_{l_a}$ . The loss in  $c_{l_a}$  generally is not harmful if the control surface is an aileron but affects the airplane stability adversely if the control surface is a rudder or an elevator.

The possibility of any buffeting tendency should not be overlooked in the design of a balanced control surface. Flight tests as well as wind-tunnel tests have revealed such tendencies for Frise ailerons as pointed out in reference 1. The buffeting appears to occur in the region of the negative deflections at which the air flow separates from the protruding nose; that is, at deflections near the critical values given for zero angle of attack in figure 5. An increase in angle of attack usually delays buffeting for Frise ailerons. Buffeting may also be delayed by any modification that tends to delay separation; that is, by increasing the nose radius, reducing the overhang, raising the nose, bulging the lower surface of the aileron, or providing the nose with a slot or a slat. With the possible exception of the addition of a slot or slat, all these measures tend to reduce the aerodynamic balance for small deflections.

Some buffeting was noted during tests of two models having plain-overhang balances. The oscillations were not so severe, however, as those noted for Frise balances. Because this type of balance may protrude into the air stream either above or below the airfoil surface, the deflection at which buffeting may occur would be expected to be less for either positive or negative angles of attack than for zero angle of attack.

From the foregoing discussion it may be concluded that the final selection of a control-surface nose shape must be a compromise depending on the relative importance of the various factors considered.

In the case of ailerons, the selection of overhang and nose shape may be made principally from a consideration of the value of  $C_{h\delta}$  required. The effect of  $C_{h\alpha}$  on the stick forces during a roll must be considered in the choice of  $C_{h\delta}$ , but the adjustment of the nose shape or overhang of ailerons to obtain a desired value of  $C_{h\alpha}$  is not recommended. A nose shape similar to type B seems the most promising of those tested; therefore, for original design work, it should generally be necessary to determine only the overhang for a nose shape of type B required to give a value of  $C_{h\delta}$  already decided upon. The value of  $C_{h\delta}$  actually obtained may be adjusted later within a limited range by making minor modifications to the nose shape without changing the length of overhang. The effect of nose shape on the peak pressures, the critical deflection, and the variation of  $C_{h\delta}$  with deflection, however, must be given consideration.

The hinge-moment parameters  $C_{h\delta}$  and  $C_{h\alpha}$  are of almost equal importance for tail surfaces, and the selection of the overhang and nose shape therefore depends on obtaining desirable values for each of these parameters. As has already been pointed out, the nose shape has little effect on  $C_{h\alpha}$  provided the gap is sealed. The overhang may consequently be selected to obtain the desired value of  $C_{h\alpha}$  and the nose shape may then be selected to obtain the desired value of  $C_{h\delta}$ , due consideration being taken of the effect of nose shape on the peak pressure, on the critical deflection, and on the variation of  $C_{h\delta}$  with deflection. If the desired value of  $C_{h\delta}$  cannot be obtained by selection of only the nose shape, some adjustment of the overhang may be necessary, and compromise values of  $C_{h\delta}$  and  $C_{h\alpha}$  will thereby be obtained.

## COMPARISON OF RESULTS WITH THEORY

The faired curve of figure 2(b) and the theoretical values of  $ch_\delta$  for plain sealed flaps derived by Glauert and presented in references 29 and 30 were used in computing the hinge moments of flaps with plain sealed overhangs on an infinitely thin airfoil, for which  $K_1$  reduces to  $(c_b/c_f)^2$ . The values thus computed were then compared with theoretically derived values presented in figure 5 of reference 31. The data of reference 31 are presented for values of the over-all control-surface chord  $(c_b + c_f)$  equal to  $0.25c$  and  $0.50c$  with various hinge locations for several values of a parameter  $\lambda$ . In reference 31,  $\lambda$  is an effective reduction in balance chord and is the distance over which the concentrated source-sink representing the steep break at the balance nose is spread in order to picture the local flow and at the same time retain physical reality. According to reference 31,  $\lambda$  is probably greater than 5 percent and less than 40 percent of the balance chord for airfoils of finite thickness. The values for an infinitely thin airfoil would be expected to fall near the lower limit of the suggested range of  $\lambda$ . This premise is borne out by a comparison of the theoretical curves and the experimental data extrapolated to zero thickness in the manner noted. The experimental data forms a curve located at  $\lambda = 0.03$  to  $0.05$  for both values of over-all control surface chord.

## DESIGN PROCEDURE

The results of the present analysis are considered applicable to the original design of control-surface balances and of balance modifications for control surfaces already in use. The procedure recommended for an original design will be illustrated in detail by an example:

Let it be required to estimate the length of plain overhang for a nose shape of type B to give a final value of  $ch_\delta$  of  $-0.0010$  for a  $0.20c$  aileron on an NACA 23012 airfoil. The aerodynamic characteristics needed in the design are: (1) the slope  $ch_\delta$  of the

plain unbalanced aileron having the same gap condition as the proposed balanced aileron, and (2) the average slope of the lift curve over the aileron portion of the wing  $C_{L1\alpha}$

Because only the increments of slopes due to the balance are considered in the present correlation of hinge-moment characteristics, the ability to obtain a desired value of  $C_{h\delta}$  for the balanced control surface is critically dependent upon the accuracy of the value of  $C_{h\delta}$  used as a base. The value of this base may be estimated from comparable finite-span data or calculated from section data, but the final value of  $C_{h\delta}$  obtained for the balanced aileron cannot be expected to be more accurate than the value used for the base. The slope of the lift curve of the entire surface  $C_{L\alpha}$  will usually be known from experimental data. The average slope over the span of the aileron  $C_{L1\alpha}$  may be estimated with sufficient accuracy by the method of reference 1.

It is assumed that the following results were obtained:

$$C_{h\delta} \text{ (for plain unbalanced aileron) } = -0.0070$$

$$C_{L1\alpha} = 0.080$$

The increment of hinge-moment slope required of the plain-overhang balance is

$$\Delta C_{h\delta} = -0.0010 - (-0.0070) = 0.0060$$

and therefore

$$\frac{\Delta C_{h\delta}}{C_{L1\alpha}} = \frac{0.0060}{0.080} = 0.075$$

For finite-span ailerons the balance factor  $K_1$  is equal

to  $\frac{\Delta C_{h\delta}}{C_{L1\alpha}}$  (fig. 2); thus,

$$K_1 = 0.075$$

The required overhang for a nose shape of type B may now be determined approximately from figure 3(a), by use of the value of  $K_1$  just determined and

$\frac{t/2}{c_f} = 0.131$  from the known airfoil ordinates at the aileron hinge line. Therefore,

$$\frac{\bar{c}_b}{\bar{c}_f} = 0.397$$

The accuracy of this value may be checked by drawing the aileron nose to the proper ordinates (balance 1 of fig. 14) from which the contour-balance chord may be obtained graphically. For constant-percentage-chord ailerons, the result is

$$\frac{\bar{c}_b'}{\bar{c}_f} = 0.221$$

Now, from figure 1,  $F_1 = 0.141$ ,  $F_2 = 0.521$ , and therefore  $K_1 = 0.074$ , which is sufficiently close to the value required. As has already been shown, the value of  $\bar{c}_b/\bar{c}_f$  obtained from figure 3 may be accepted as the final value for nose shapes of type A, B, or D for any airfoil of the NACA conventional four-digit or five-digit series and, therefore, the check just performed was not necessary in this instance. If an airfoil section having a different thickness distribution had been used, or if it had been desired to use a nose shape other than type A, B, or D, figure 3 would still have been used, but only to obtain a preliminary estimate of  $\bar{c}_b/\bar{c}_f$ .

The procedure to be used in connection with proposed modifications to plain-overhang balances is similar to that just outlined for an original design except that the value of  $C_{h_8}$  of the original balanced control surface may be used as the base. If only a certain increment  $\Delta C_{h_8}$  is desired, no base value is necessary.

In order to illustrate the change in overhang that would normally be required to give the same amount of aerodynamic balance for small deflections when the nose radii are varied, two additional nose shapes have been derived and are presented in figure 14(a). Balance 2 has one and one-half times the nose radius of balance 1 and balance 3 has one half the nose radius of balance 1. The geometric constants of the three balances are tabulated in figure 14(a).

The variation of  $C_{h_8}$  that may be expected to accompany moderate changes in the nose radius with a fixed overhang is indicated in figure 14(b). The estimated values of  $C_{h_8}$  range from -0.0022 to 0.0002.

The recommended procedure for the design or modification of control surfaces with Frise balances is similar to that just outlined for plain-overhang balances except that the increment  $\Delta C_{h_8}$  applies only to the negative deflection range. The slope  $C_{h_8}$  for positive deflections greater than about  $8^\circ$  may be considered to be unaffected by overhang or nose shape. The complete hinge-moment curve can be approximated with a fair degree of accuracy at low angles of attack by fairing a curve between the balanced negative portion (tangent at  $\delta_f \approx -2^\circ$ ) and the unbalanced positive portion (tangent at  $\delta_f \approx 8^\circ$ ). The exact location of the curve with respect to the axes is dependent on a number of factors, however, including the shape of the airfoil section. A prediction of the characteristics of a control surface with a Frise balance, therefore, cannot be expected to be as accurate as a prediction for a control surface with a plain-overhang balance. It is believed, however, that the effect of minor modifications to either plain-overhang or Frise balances can be predicted with fair accuracy by the method outlined.

## CONCLUSIONS

The results of the preceding correlation and analysis indicate the following general conclusions regarding control surfaces having plain-overhang or Frise balances:

1. The effects of balance variations in changing the slope of the curve of hinge-moment coefficient plotted against control-surface deflection and in changing the lift effectiveness of the control surface could be correlated for various models at low Mach numbers by the use of a balance factor that accounted for the size and shape of the overhang.

2. No correlation factor was obtained that would adequately account for all the variables which affect the slope of the curve of hinge-moment coefficient plotted against angle of attack or which affect the deflection range over which the balance is effective in reducing the slope of the hinge-moment curve.

3. The presence of a small gap at the nose of a plain-overhang balanced flap and of the corresponding unbalanced flap does not appreciably alter the differences in the slopes of the curves of hinge moment plotted against control deflection.

4. The shape of the balance nose varied the effect of a gap at the control leading edge on the slope of the curve of hinge moment plotted against angle of attack for plain-overhang balances.

5. The presence of a gap at the control leading edge consistently increased the effect of overhang in increasing the control lift-effectiveness parameter. With the open gap the increase in the lift-effectiveness parameter with increase in overhang was caused by an increase in the slope of the curve of lift plotted against control-surface deflection and a decrease in the slope of the curve of lift plotted against angle of attack.



6. The data were too meager to justify any definite generalizations concerning the effects of Mach number on plain-overhang and Frise balances except that increases in Mach number consistently decreased the deflection range over which the balance was effective in reducing the slope of the hinge-moment curve.

Langley Memorial Aeronautical Laboratory,  
National Advisory Committee for Aeronautics,  
Langley Field, Va.,

## REFERENCES

1. Rogallo, F. M.: Collection of Balanced-Aileron Test Data. NACA ACR No. 4A11, 1944.
2. Sears, Richard I.: Wind-Tunnel Data on the Aerodynamic Characteristics of Airplane Control Surfaces. NACA ACR No. 3E08, 1943.
3. Rogallo, F. M., and Lowry, John G.: Résumé of Data for Internally Balanced Ailerons. NACA RE, March 1943.
4. Purser, Paul E., and Gillis, Clarence L.: Preliminary Correlation of the Effects of Beveled Trailing Edges on the Hinge-Moment Characteristics of Control Surfaces. NACA CB No. 3E14, 1943.
5. Lowry, John G.: Résumé of Hinge-Moment Data for Unshielded Horn-Balanced Control Surfaces. NACA RB No. 3F19, 1943.
6. Jacobs, Eastman N., Abbott, Ira H., and Davidson, Milton: Supplement (loose-leaf) to NACA Advance Confidential Report, Preliminary Low-Drag-Airfoil and Flap Data from Tests at Large Reynolds Numbers and Low Turbulence. NACA, March 1942, p. 21a.
7. Letko, W., Hollingworth, T. A., and Anderson, R. A.: Wind-Tunnel Tests of Ailerons at Various Speeds. IV - Ailerons of 0.20 Airfoil Chord and True Contour with 0.35 Aileron-Chord Extreme Blunt-Nose Balance on the NACA 23012 Airfoil. NACA ACR No. 3H28, 1943.
8. Letko, W., Denaci, H. G., and Freed, C.: Wind-Tunnel Tests of Ailerons at Various Speeds. I - Ailerons of 0.20 Airfoil Chord and True Contour with 0.35 Aileron-Chord Extreme Blunt Nose Balance on the NACA 66,2-216 Airfoil. NACA ACR No. 3F11, 1943.
9. Sears, Richard I.: Wind-Tunnel Investigation of Control-Surface Characteristics. I - Effect of Gap on the Aerodynamic Characteristics of an NACA 0009 Airfoil with a 30-Percent-Chord Plain Flap. NACA ARR, June 1941.

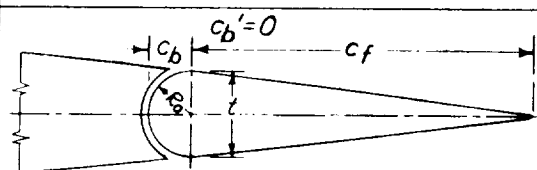
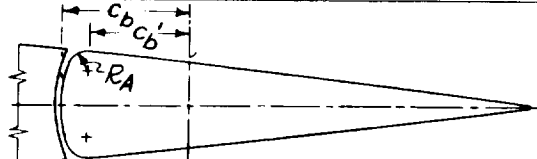
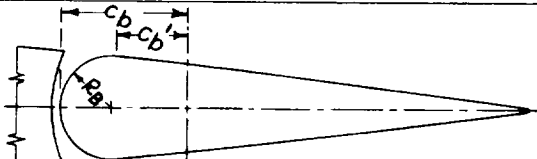
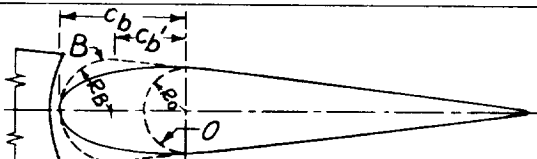
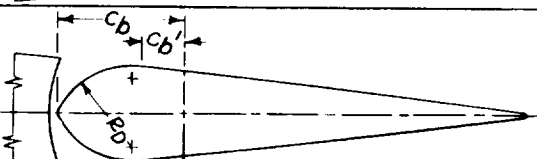
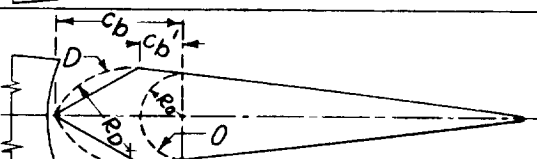
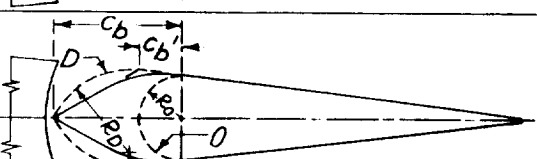
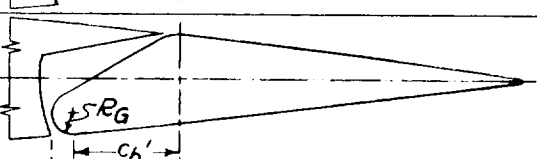
10. Ames, Milton B., Jr.: Wind-Tunnel Investigation of Control-Surface Characteristics. III - A Small Aerodynamic Balance of Various Nose Shapes Used with a 30-Percent-Chord Flap on an NACA 0009 Airfoil. NACA ARR, Aug. 1941.
11. Ames, Milton B., Jr., and Eastman, Donald R., Jr.: Wind-Tunnel Investigation of Control-Surface Characteristics. IV - A Medium Aerodynamic Balance of Various Nose Shapes Used with a 30-Percent-Chord Flap on an NACA 0009 Airfoil. NACA ARR, Sept. 1941.
12. Sears, Richard I., and Hoggard, H. Page, Jr.: Wind-Tunnel Investigation of Control-Surface Characteristics. II - A Large Aerodynamic Balance of Various Nose Shapes with a 30-Percent-Chord Flap on an NACA 0009 Airfoil. NACA ARR, Aug. 1941.
13. Gillis, Clarence L., and Lockwood, Vernard E.: Wind-Tunnel Investigation of Control-Surface Characteristics. XIII - Various Flap Overhangs Used with a 30-Percent-Chord Flap on an NACA 66-009 Airfoil. NACA ACR No. 3G20, 1943.
14. Sears, Richard I., and Liddell, Robert B.: Wind-Tunnel Investigation of Control-Surface Characteristics. VI - A 30-Percent-Chord Plain Flap on the NACA 0015 Airfoil. NACA ARR, June 1942.
15. Sears, Richard I., and Hoggard, H. Page, Jr.: Wind-Tunnel Investigation of Control-Surface Characteristics. VII - A Medium Aerodynamic Balance of Two Nose Shapes Used with a 30-Percent-Chord Flap on an NACA 0015 Airfoil. NACA ARR, July 1942.
16. Sears, Richard I., and Gillis, Clarence L.: Wind-Tunnel Investigation of Control-Surface Characteristics. VIII - A Large Aerodynamic Balance of Two Nose Shapes Used with a 30-Percent-Chord Flap on an NACA 0015 Airfoil. NACA ARR, July 1942.
17. Hoggard, H. Page, Jr.: Wind-Tunnel Investigation of Control-Surface Characteristics. X - A 30-Percent-Chord Plain Flap with Straight Contour on the NACA 0015 Airfoil. NACA ARR, Sept. 1942.

18. Sears, Richard I., and Hoggard, H. Page, Jr.: Wind-Tunnel Investigation of Control-Surface Characteristics. XI - Various Large Overhang and Internal-Type Aerodynamic Balances for a Straight Contour Flap on the NACA 0015 Airfoil. NACA ARR, Jan. 1943.
19. Purser, Paul E., and Toll, Thomas A.: Wind-Tunnel Investigation of the Characteristics of Blunt-Nose Ailerons on a Tapered Wing. NACA ARR, Feb. 1943.
20. Sears, Richard I., and Hoggard, H. Page, Jr.: Characteristics of Plain and Balanced Elevators on a Typical Pursuit Fuselage at Attitudes Simulating Normal-Flight and Spin Conditions. NACA ARR, March 1942.
21. Goett, Harry J., and Reeder, J. P.: Effects of Elevator Nose Shape, Gap, Balance, and Tabs on the Aerodynamic Characteristics of a Horizontal Tail Surface. NACA Rep. No. 675, 1939.
22. Letko, W., and Kemp, W. B.: Wind-Tunnel Tests of Ailerons at Various Speeds. III - Ailerons of 0.20 Airfoil Chord and True Contour with 0.35-Aileron-Chord Frise Balance on the NACA 23012 Airfoil. NACA ACR No. 3114, 1943.
23. Holtzclaw, Ralph W., and Erickson, Myles D.: Wind-Tunnel Investigation of Flap, Aileron, and Exterior Bomb Installations on a 24-Inch Constant-Chord North American XB-28 Wing Model. NACA ARR, July 1942.
24. Rogallo, F. M., and Purser, Paul E.: Wind-Tunnel Investigation of 20-Percent-Chord Plain and Frise Ailerons on an NACA 23012 Airfoil. NACA ARR, Dec. 1941.
25. Jacobs, Eastman N., Pinkerton, Robert M., and Greenberg, Harry: Tests of Related Forward-Camber Airfoils in the Variable-Density Wind Tunnel. NACA Rep. No. 610, 1937.

26. Letko, W., and Denaci, H. G.: Wind-Tunnel Tests of Ailerons at Various Speeds. V - Pressure Distributions over the NACA 66,2-216 and NACA 23012 Airfoils with Various Balances on 0.20-Chord Ailerons. NACA ACR No. 3W05, 1943.
27. Dingeldein, Richard C.: Full-Scale Tunnel Investigation of the Pressure Distribution over the Tail of the P-47B Airplane. NACA ARR No. 3E25, 1943.
28. LeBeck, Robert K.: 20-Foot Wind Tunnel Pressure Distribution Measurements on the Full-Scale Tail Surfaces of the Republic P-47B Airplane - Test No. 14. AAF T.R. No. 4926, Materiel Command, Army Air Forces, May 13, 1943.
29. Glauert, H.: Theoretical Relationships for an Aerofoil with Hinged Flap. R. & M. No. 1095, British A.R.C., 1927.
30. Ames, Milton B., Jr., and Sears, Richard I.: Determination of Control-Surface Characteristics from NACA Flap-Flap and Tab Data. NACA Rep. No. 721, 1941.
31. Theodorsen, Theodore, and Garrick, I. E.: Non-stationary Flow about a Wing-Aileron-Tab Combination Including Aerodynamic Balance. NACA Rep. No. 736, 1942.



TABLE I.- VARIOUS NOSE SHAPES CONSIDERED IN  
CORRELATION OF PLAIN-OVERHANG AND FRISE BALANCES  
AND CORRESPONDING EXPRESSIONS FOR NOSE-SHAPE FACTOR.

Nose type	Section showing nose shape	Nose-shape factor, $F_2'$
O		$1 - \sqrt{1 - \left( \frac{1 + \bar{c}_b/\bar{c}_f}{1 + \bar{c}_b/\bar{c}_f} \right)^2}$
A		$1 - \sqrt{1 - \left( \frac{1 + \bar{c}_b'/\bar{c}_f}{1 + \bar{c}_b/\bar{c}_f} \right)^2}$
B		$1 - \sqrt{1 - \left( \frac{1 + \bar{c}_b'/\bar{c}_f}{1 + \bar{c}_b/\bar{c}_f} \right)^2}$
C		$\left( \frac{M_C - M_O}{M_B - M_O} \right)^{1.4} \left( 1 - \sqrt{1 - \left( \frac{1 + \bar{c}_b'/\bar{c}_f}{1 + \bar{c}_b/\bar{c}_f} \right)^2} \right)$
D		$1 - \sqrt{1 - \left( \frac{1 + \bar{c}_b'/\bar{c}_f}{1 + \bar{c}_b/\bar{c}_f} \right)^2}$
E		$\left( \frac{M_E - M_O}{M_D - M_O} \right)^{0.7} \left( 1 - \sqrt{1 - \left( \frac{1 + \bar{c}_b'/\bar{c}_f}{1 + \bar{c}_b/\bar{c}_f} \right)^2} \right)$
F		$\left( \frac{M_F - M_O}{M_D - M_O} \right)^{0.7} \left( 1 - \sqrt{1 - \left( \frac{1 + \bar{c}_b'/\bar{c}_f}{1 + \bar{c}_b/\bar{c}_f} \right)^2} \right)$
G		$1 - \sqrt{1 - \left( \frac{1 + \bar{c}_b'/\bar{c}_f}{1 + \bar{c}_b/\bar{c}_f} \right)^2}$





L-665

Table II.- INFORMATION REGARDING TESTS OF MODELS HAVING BALANCED CONTROL SURFACES

A - CONTROL SURFACES WITH EXPOSED-OVERHANG BALANCES

[Designations of low-drag airfoils, regardless of the form in which they appear in the other references, are changed throughout to the form prescribed on p. 21a of reference 6.]

NATIONAL ADVISORY  
COMMITTEE FOR AERONAUTICS.

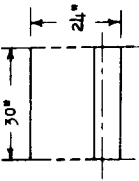
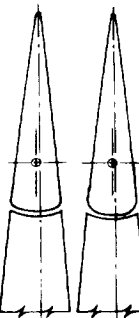
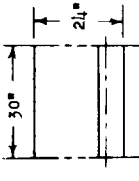
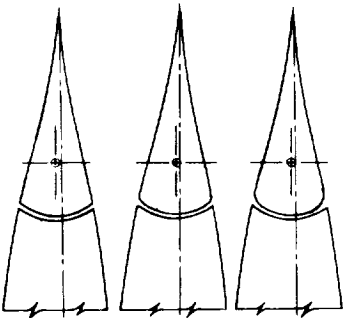
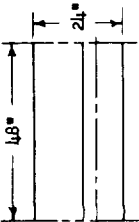
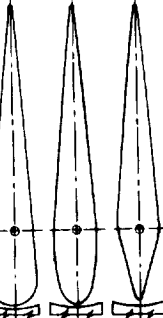
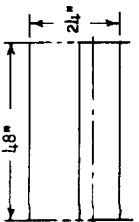
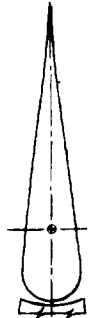
Model		Typical section of control surface	Airfoil section	A	$\lambda$	$\bar{c}_r/\bar{c}$	$\bar{c}_y/\bar{c}_r$	Gap	Type of test	Reference
Sym- bol	Designation									
⊙	I			$\infty$	---	0.20	0.35	$\left\{ \begin{array}{l} \text{Sealed} \\ 0.0005c \\ 0.0030c \\ 0.0055c \\ 0.0107c \end{array} \right\}$	Two-dimensional	7
△	II			$\infty$	---	0.20	0.35	$\left\{ \begin{array}{l} \text{Sealed} \\ 0.0005c \\ 0.0030c \\ 0.0055c \\ 0.0107c \end{array} \right\}$	Two-dimensional	8
□	III			$\infty$	---	0.30	$\left\{ \begin{array}{l} 0.092 \\ 0.200 \\ 0.350 \\ 0.495 \end{array} \right\}$	$\left\{ \begin{array}{l} \text{Sealed} \\ 0.0010c \\ 0.0015c \\ 0.0050c \\ 0.0100c \end{array} \right\}$	Two-dimensional	9, 10, 11, 12
▽	IV			$\infty$	---	0.30	$\left\{ \begin{array}{l} 0.113 \\ 0.350 \\ 0.500 \end{array} \right\}$	$\left\{ \begin{array}{l} \text{Sealed} \\ 0.005c \end{array} \right\}$	Two-dimensional	13



Table II.- INFORMATION REGARDING TESTS OF MODELS HAVING BALANCED CONTROL SURFACES - Continued

A - CONTROL SURFACES WITH KIPPER-OFFSHAW BALANCES - Continued

NATIONAL ADVISORY  
COMMITTEE FOR AERONAUTICS.

[Designations of low-drag airfoils, regardless of the form in which they appear in the other references, are changed throughout to the form prescribed on p. 21a of reference 6.]

Model		Typical section of control surface	Airfoil section	$\Lambda$	$\lambda$	$\bar{c}_l/\bar{c}$	$\bar{c}_l/\bar{c}_r$	Gap	Type of test	Refer- ence
Sym- bol	Des- igna- tion									
	V		Modified NACA 66-009 (straight-contour flap)	$\infty$	---	0.26	0.30	{ Sealed 0.0010	Two-dimensional	----
	VI		NACA 0015	$\infty$	---	0.30	{ 0.153 .350 .500	{ Sealed 0.0050	Two-dimensional	14, 15
	VII		Modified NACA 0015 (straight-contour flap)	$\infty$	---	0.30	{ 0.153 .350 .500	{ 0.0050	Two-dimensional	17, 18



L-665

Table 11.- INFORMATION REGARDING TESTS OF MODELS HAVING BALANCED CONTROL SURFACES - Continued

A - CONTROL SURFACES WITH EXPOSED-OVERHANG BALANCES - Continued

[Designations of low-drag airfoils, regardless of the form in which they appear in the other references, are changed throughout to the form prescribed on p. 21a of reference 6]

NATIONAL ADVISORY  
COMMITTEE FOR AERONAUTICS.

Sym- bol	Des- igna- tion	Model		Typical section of control surface	Airfoil section		$\lambda$	$\bar{x}_2/\bar{c}$	$\bar{x}_b/\bar{c}_f$	Gap	Type of test	Refer- ence
		Plan form of surface			Root.	Tip.						
▽	VIII				Root, NACA 23015	Tip, NACA 4412	7.2	$\begin{cases} 0.195 \\ 0.206 \end{cases}$	$\begin{cases} 0.400 \\ 0.322 \end{cases}$	$\begin{cases} 0.0025c \\ 0.0025c \end{cases}$	Complete model	---
◁	IX				Root, NACA 23015.5 (approx.)	Tip, NACA 23008.25 (approx.)	5.6	0.60	$\begin{cases} 0.113 \\ 0.200 \\ 0.400 \end{cases}$	$\begin{cases} \text{Sealed} \\ 0.005c \end{cases}$	Semi-span wing model	19
▷	X				Root, NACA 44223-22265219-119 $a = 1.0$	Tip, NACA 44223-22265219-119 $a = 0.5$	$a = 12.0$	$a = 0.32$	0.35	0.005c	Quarter-span wing model	---
+	XI				NACA 0009		3.7	0.57	$\begin{cases} 0.090 \\ 0.350 \\ 0.500 \end{cases}$	$\begin{cases} \text{Sealed} \\ 0.005c \end{cases}$	Tail-surface model mounted on fuselage	20

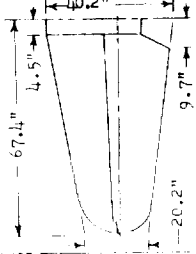

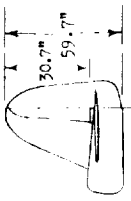

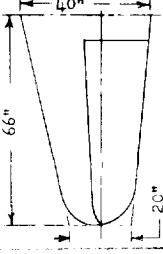

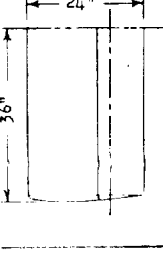
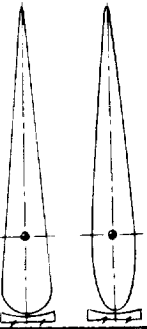
\*Values given are for complete wing and not for partial-span wing tested.



Table II.- INFORMATION REGARDING TESTS OF MODELS HAVING BALANCED CONTROL SURFACES - Continued

A - CONTROL SURFACES WITH LAPSED-OVERHANG BALANCES - Concluded

[Designations of low-drag airfoils, regardless of the form in which they appear in the other references, are changed throughout to the form prescribed on p. 21a of reference 6]

Model		Typical section of control surface	Airfoil section	A	$\lambda$	$\bar{c}_f/\bar{c}_f$	$\bar{c}_b/\bar{c}_f$	Gap	Type of test	Reference
Sym- bol	Des- ignation									
XII			NACA 0009	4.7	0.50	0.45	$\left\{ \begin{array}{l} 0.10 \\ 0.20 \end{array} \right\}$	$\left\{ \begin{array}{l} 0.005e \\ 0.005e \end{array} \right\}$	Isolated full-scale tail surface	21
XIII			Modified NACA 66-series	2.41	----	0.40	$\left\{ \begin{array}{l} 0.12 \\ 0.30 \\ 0.50 \end{array} \right\}$	$\left\{ \begin{array}{l} \text{Sealed} \\ 0.0035e \end{array} \right\}$	Tail-surface model mounted on stub fuselage	--
XIV			Tip, NACA 0009 Root, NACA 0015	4.5	0.50	$\left\{ \begin{array}{l} 0.437 \\ 0.427 \\ 0.417 \\ 0.407 \end{array} \right\}$	$\left\{ \begin{array}{l} 0.364 \\ 0.297 \\ 0.430 \\ 0.410 \end{array} \right\}$	$\left\{ \begin{array}{l} 0.0036e \\ 0.0036e \end{array} \right\}$	Semispan tail surface	--
XV			NACA 0009	3.0	1.00	0.30	$\left\{ \begin{array}{l} 0.35 \\ 0.50 \end{array} \right\}$	$\left\{ \begin{array}{l} \text{Sealed} \\ 0.005e \end{array} \right\}$	Semispan tail surface	--

NATIONAL ADVISORY  
COMMITTEE FOR AERONAUTICS.

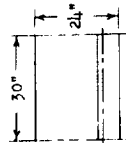
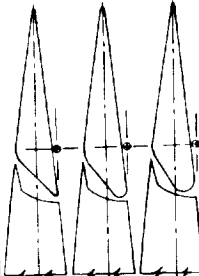


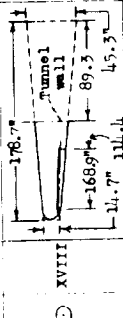
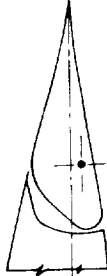
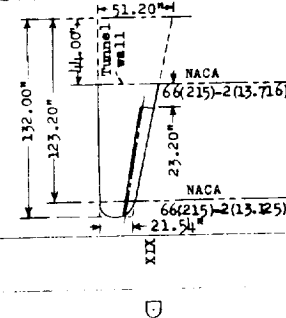
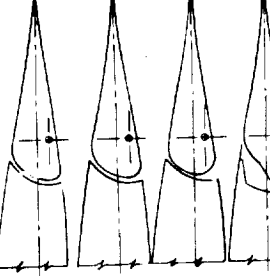
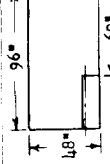





Table II.- INFORMATION REGARDING TESTS OF MODELS HAVING BALANCED CONTROL SURFACES - Continued

## B - CONTROL SURFACES WITH PRISM BALANCES

[Designations of low-drag airfoils, regardless of the form in which they appear in the other references, are changed throughout to the form prescribed on p. 21a of reference 6]

Model		Typical section of control surface	Airfoil section	$\Lambda$	$\lambda$	$\xi_r/\bar{\xi}$	$\xi_b/\xi_r$	Map	Type of test	Reference	
Sym- bol	Des- igna- tion										Plan form of surface
◇	XVI			NACA 23012	$\infty$	---	0.20	0.35	0.005c	Two-dimensional	22
◇	XVII			NACA conventional section (approx. 14 percent thick)	$\infty$	---	0.20	0.37	Open	Two-dimensional	23
◇	XVIII			Root 65(22)-22265(216)-115 $\Lambda = 1.0$ $\alpha = 0.5$	$\Lambda = 12.0$	$\lambda = 0.32$	0.23	0.42	Open	Quarter-span wing model	--
◇	XIX			NACA low-drag (See plan form)	$\Lambda = 7.3$	$\lambda = 0.42$	0.20	$\left\{ \begin{array}{l} 0.295 \\ 0.290 \\ 0.285 \\ 0.400 \end{array} \right\}$	Open	Third-span wing model	--
◇	XX			NACA 23012	4.0	1.00	0.20	$\left\{ \begin{array}{l} 0.278 \\ 0.326 \end{array} \right\}$	Open	Semispan wing model	24

\*Values given are for complete wing and not for partial-span wing tested.



L-665

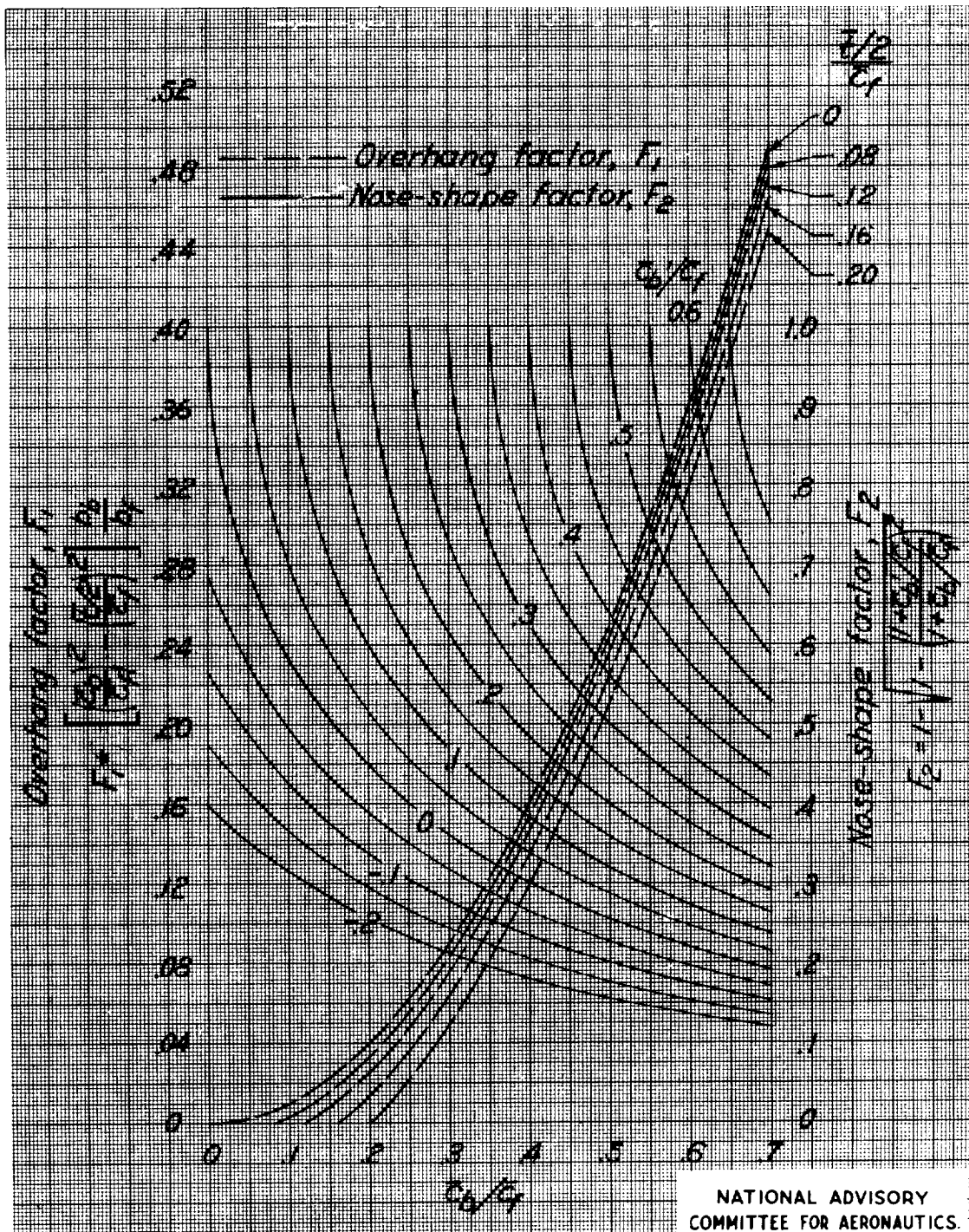


Figure 1.- Charts for determining numerical values of overhang factor and basic nose-shape factor from geometrical constants of control surfaces with plain-overhang or Frise balances.  $b_f/b_r$ , 1.0.



L-665

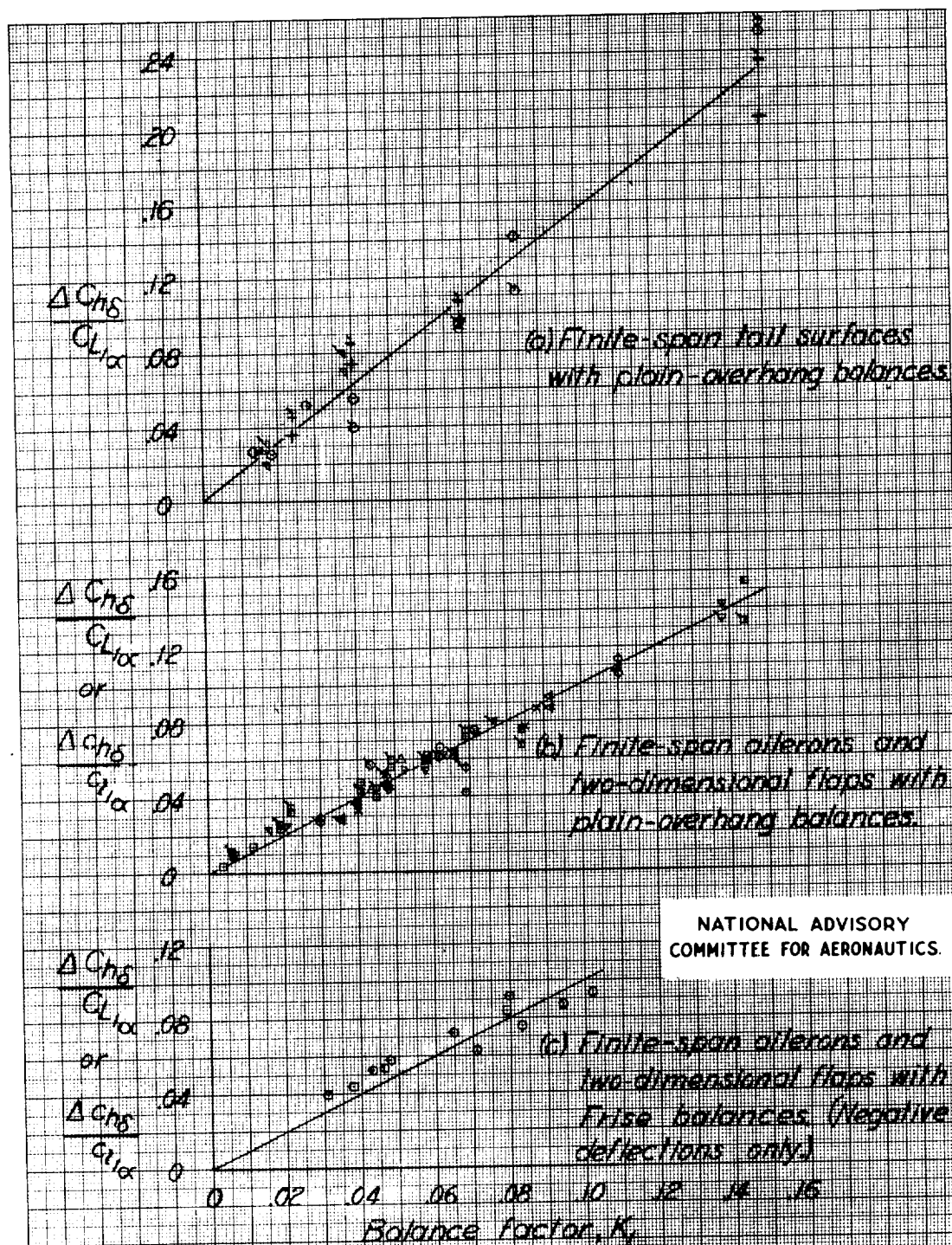
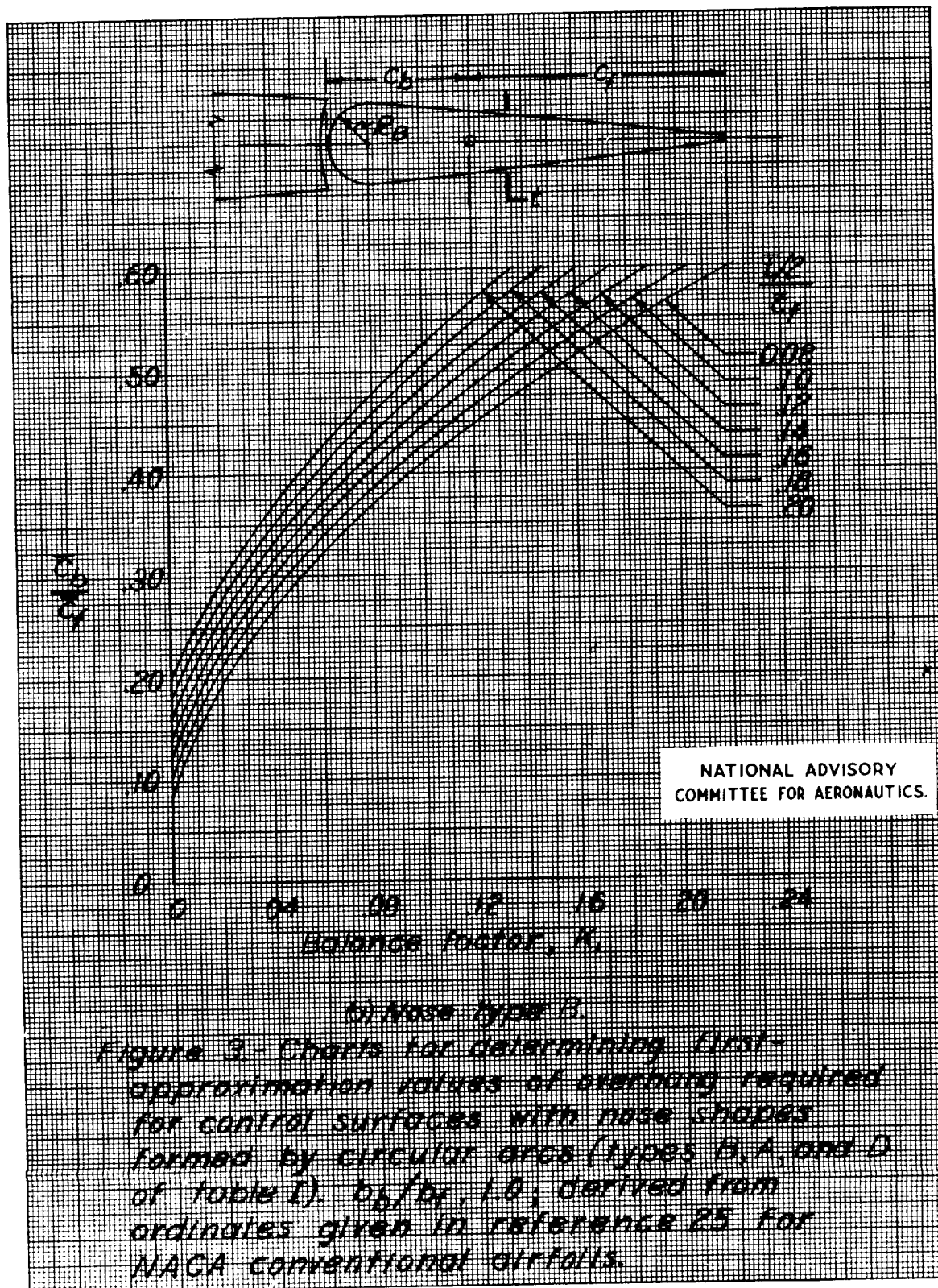


Figure 2.- Variation of  $\frac{\Delta C_{L\alpha}}{C_{L\alpha}}$  and  $\frac{\Delta C_{L\alpha}}{C_{L\alpha}}$  with balance factor for various control surfaces.  $M$ , 0.1 to 0.2; symbols are for corresponding models of table II, plain symbols, open gaps; flagged symbols, sealed gaps.

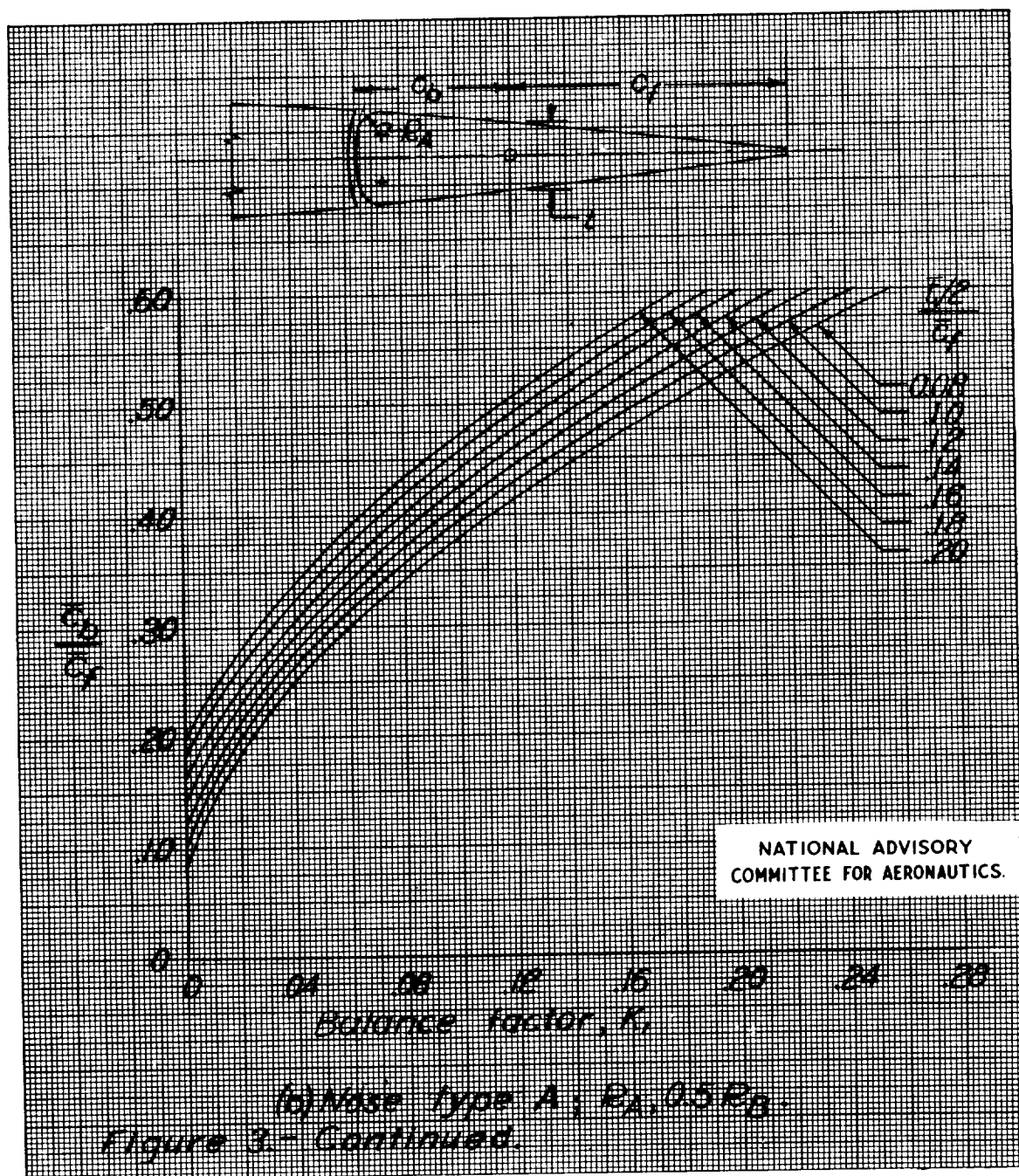






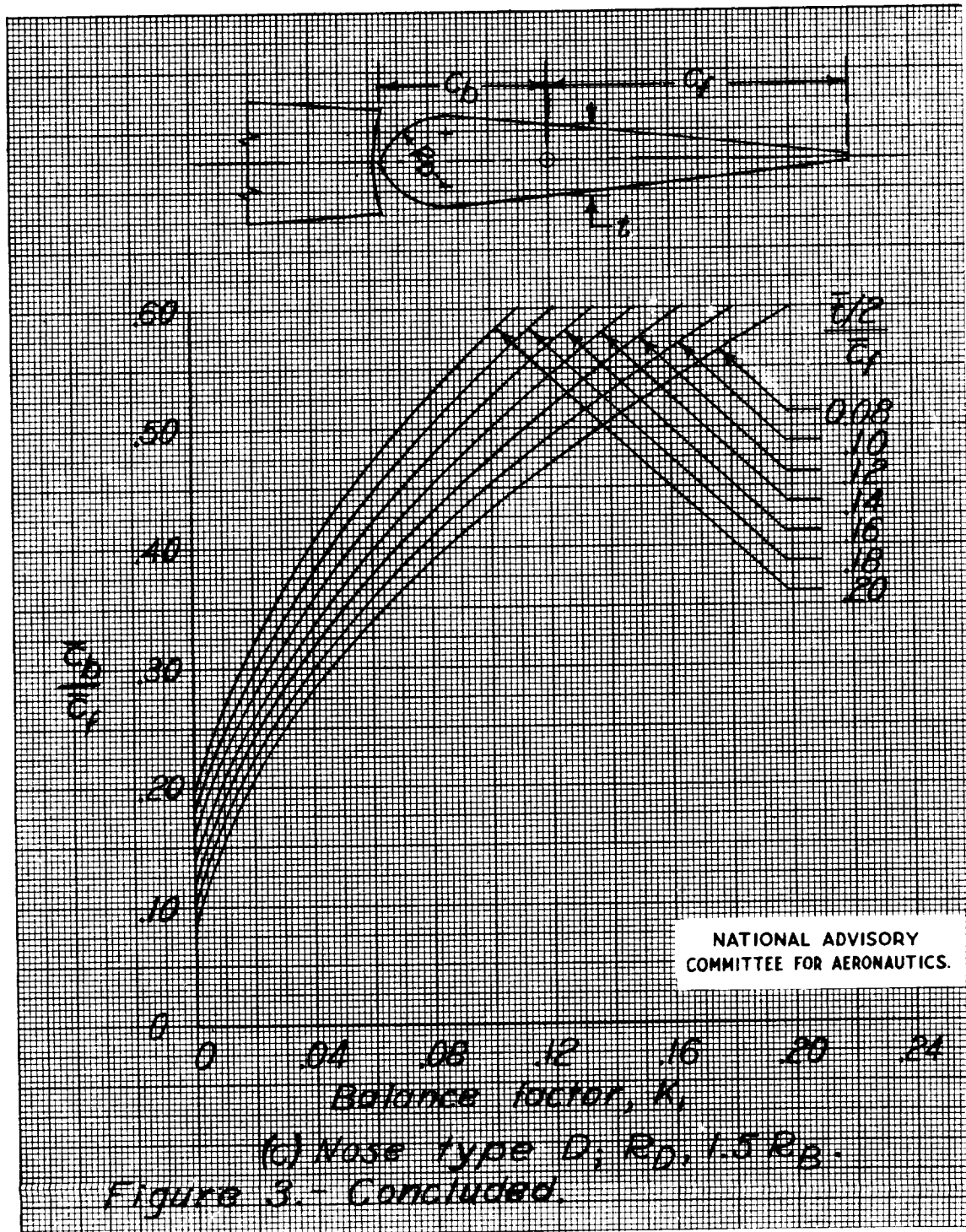


L-665





L-665





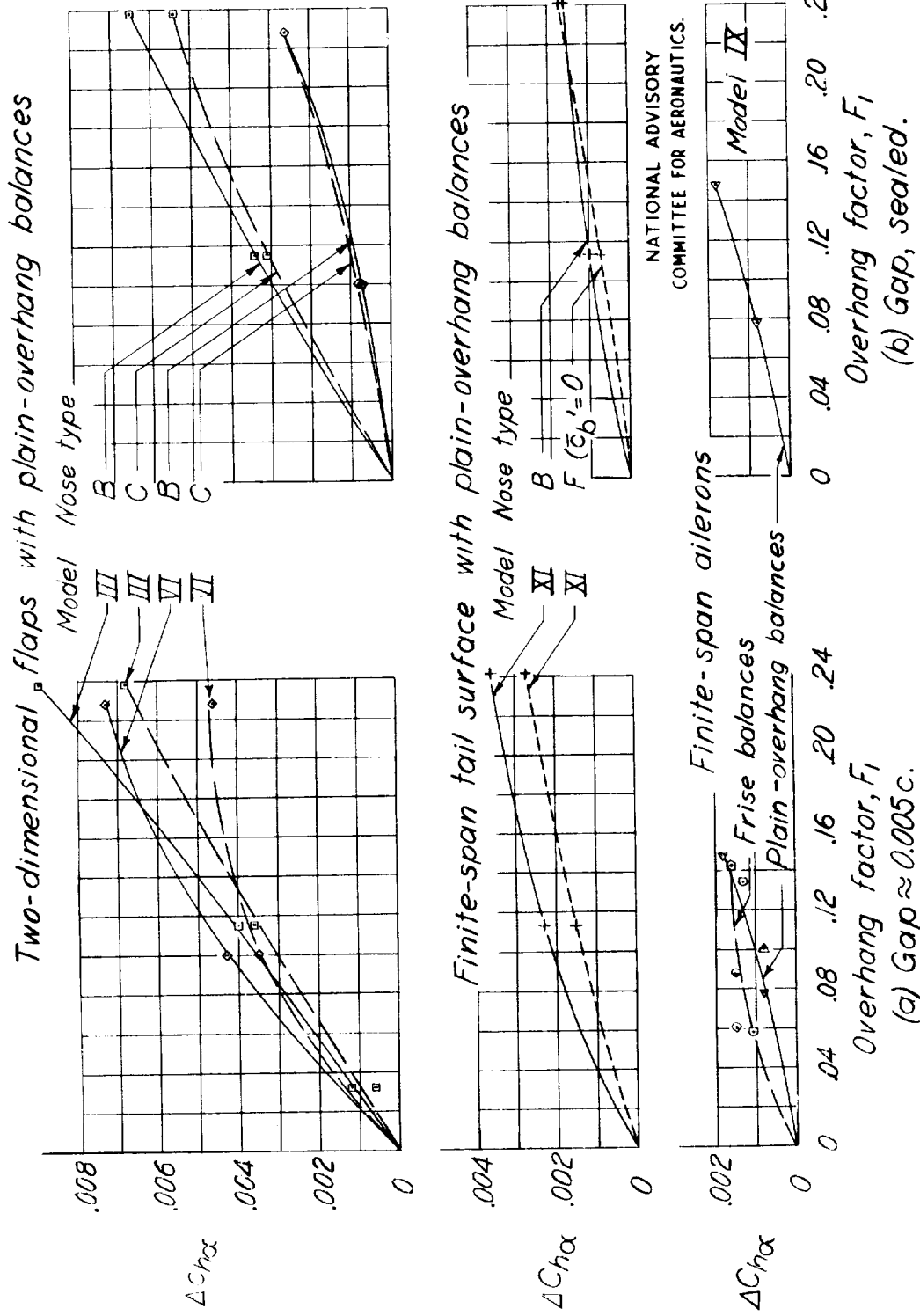


Figure 4.- Variation of increment of hinge-moment slope  $\Delta Ch_\alpha$  (or  $\Delta Ch_\alpha$ ) with overhang factor for various balanced control surfaces.  $M$ , 0.1 to 0.2.



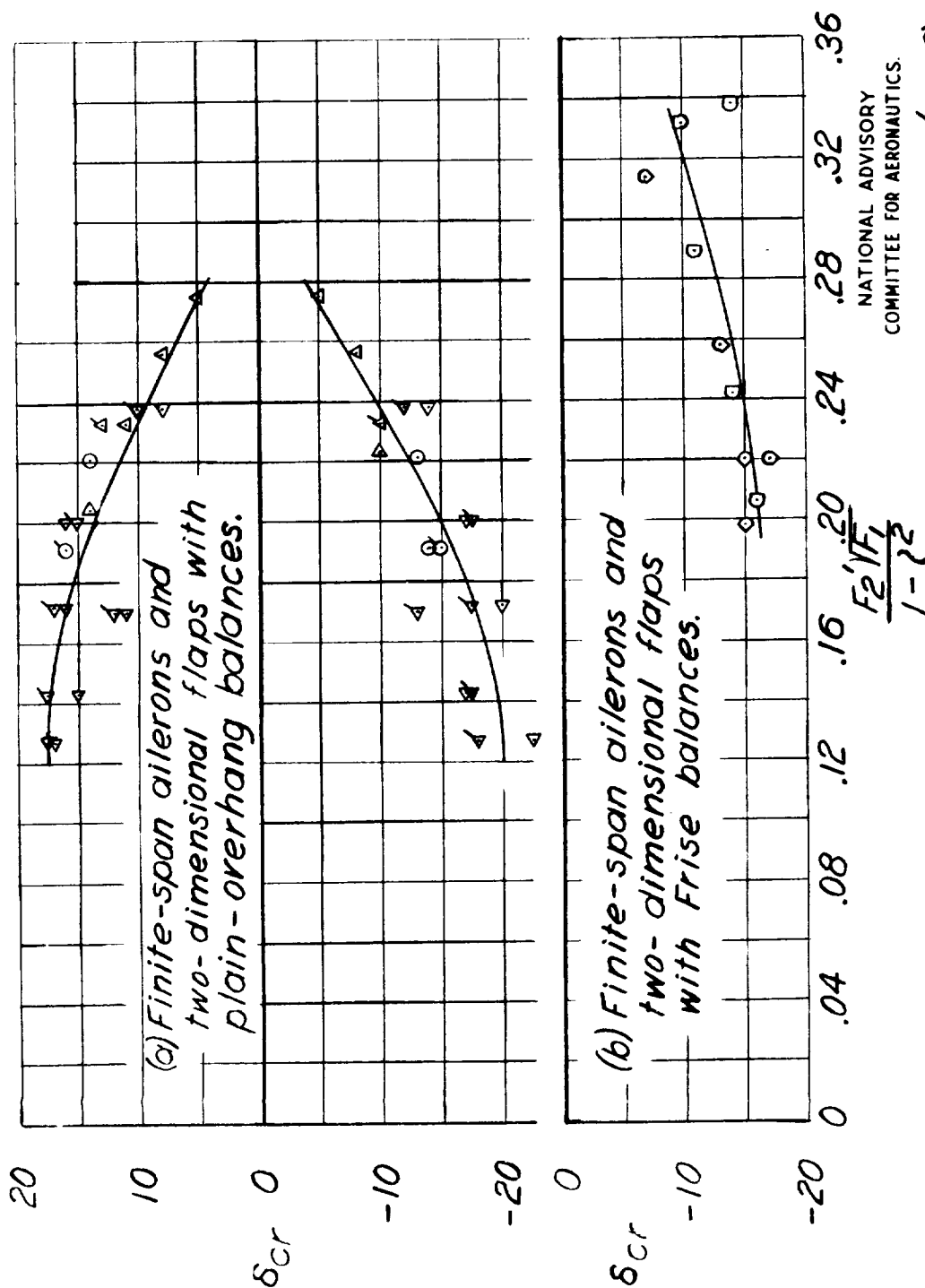


Figure 5.- Variation of critical deflection with factor  $F_2'VF_1/(1-l^2)$  for balanced control surfaces.  $M$ , 0.1 to 0.2;  $\alpha$ ,  $0^\circ$ ; symbols are for corresponding models of table II; plain symbols, open gaps; flagged symbols, sealed gaps.





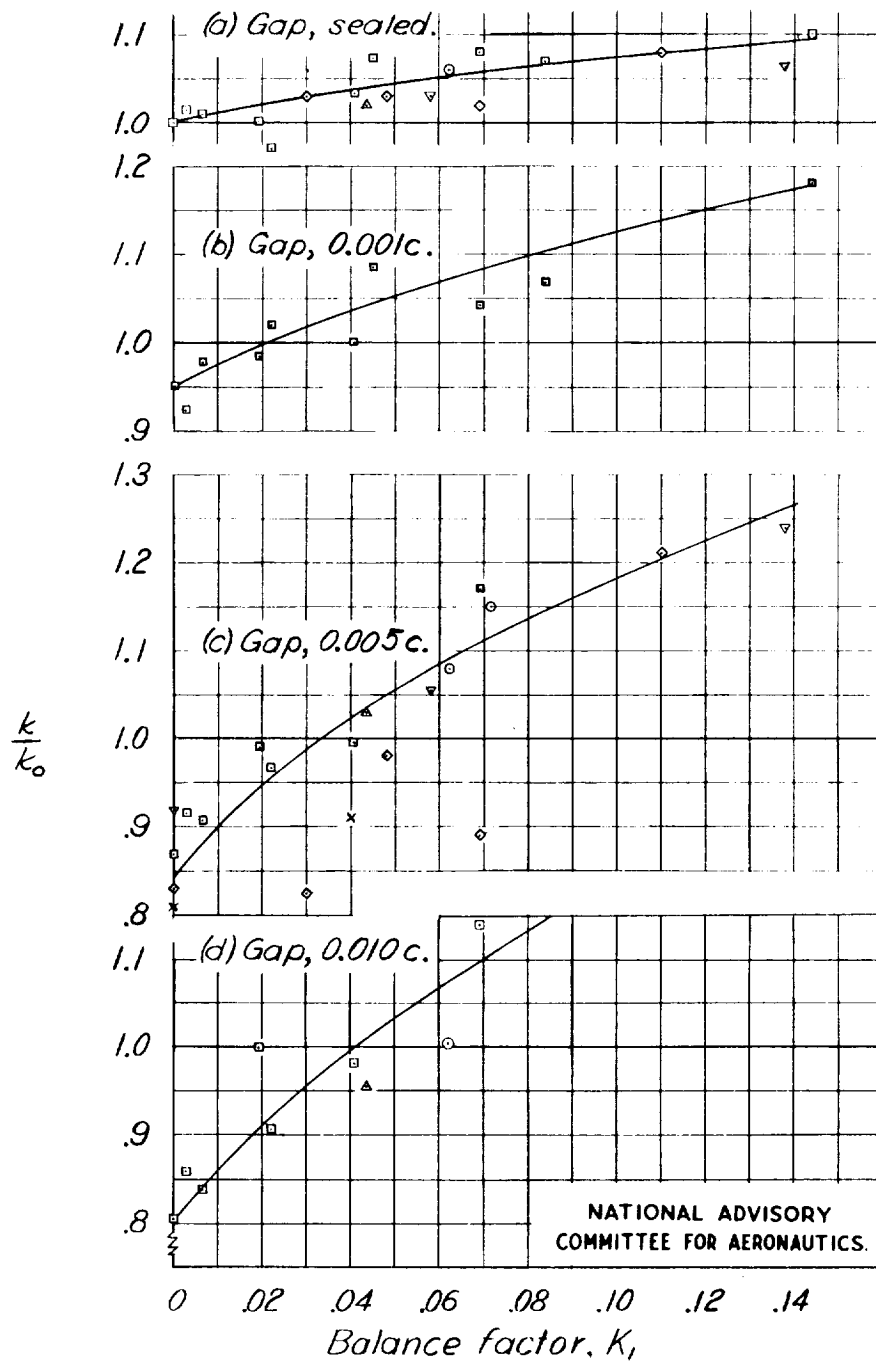


Figure 6.- Variation of lift-effectiveness parameter, relative to lift-effectiveness parameter of plain-sealed flaps, with balance factor,  $M$ , 0.1 to 0.2. Symbols are for corresponding models of table II.



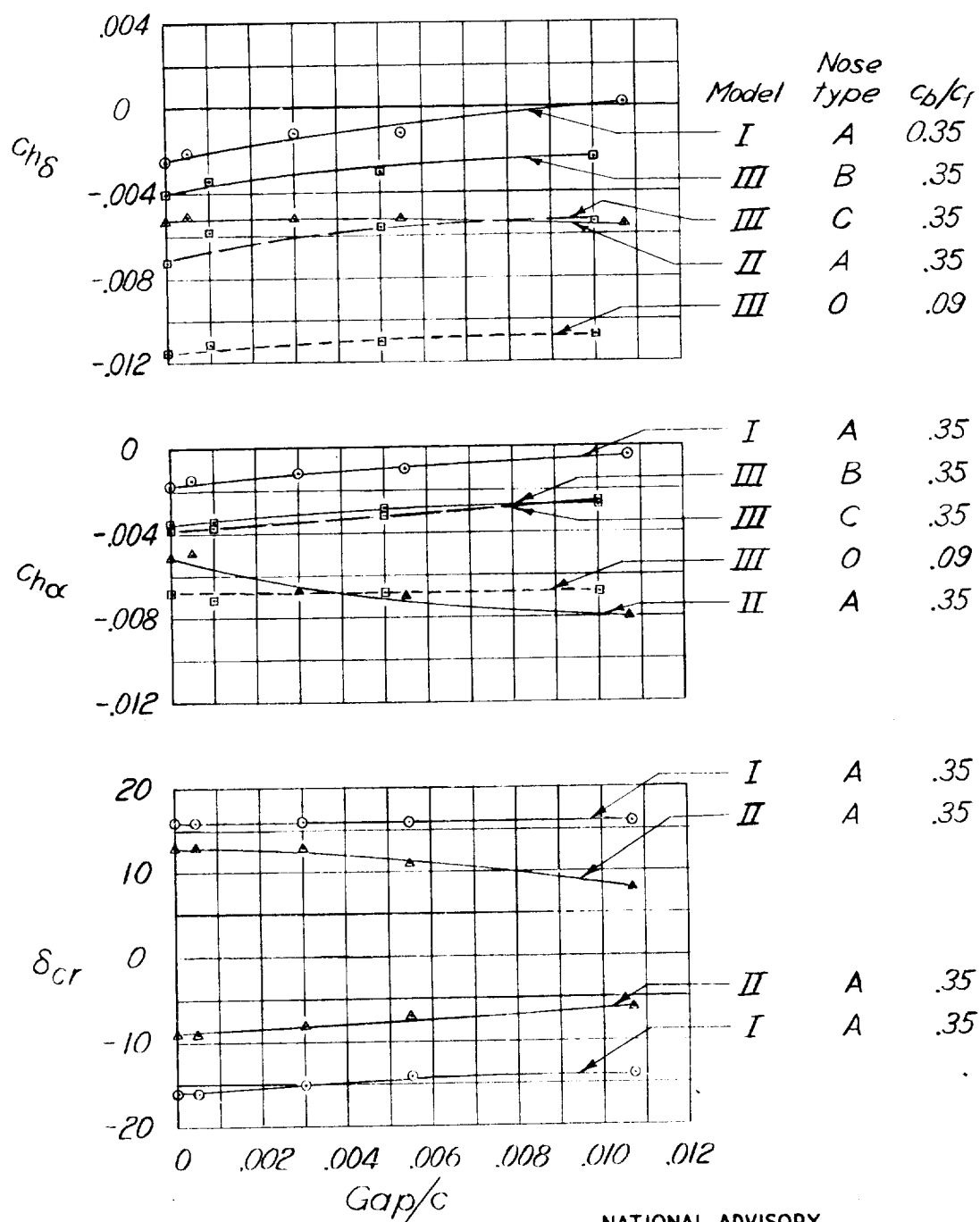
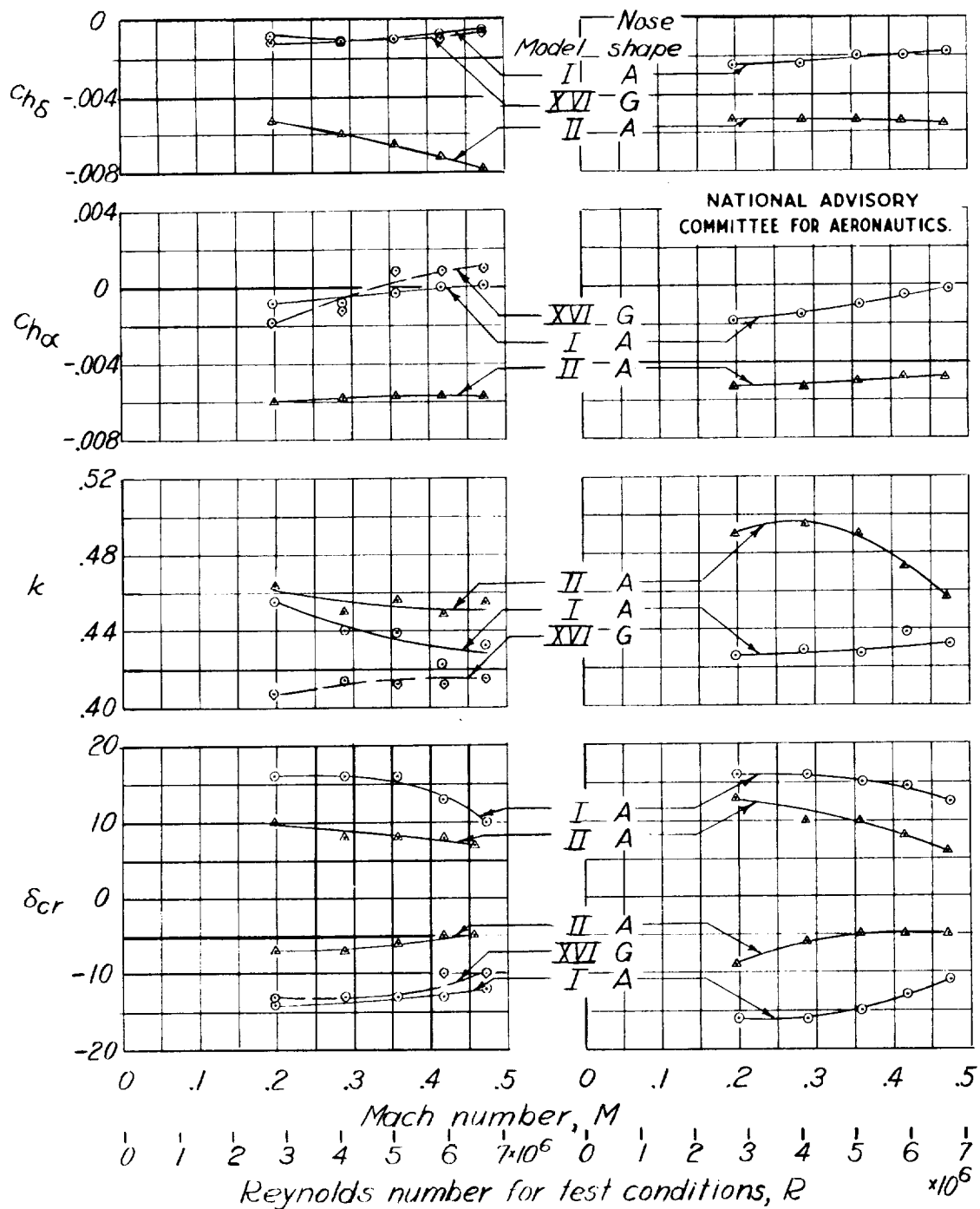


Figure 7.- Variation of flap section hinge-moment parameters and critical deflection with gap.  $\alpha, 0^\circ$ ;  $M, 0.1$  to  $0.2$ .



(a) Gap  $\approx 0.005c$ .

(b) Gap, sealed.

Figure 8.-Variation of flap section hinge-moment parameters, lift effectiveness parameter, and critical deflection with Mach number and Reynolds number.  $\alpha, 0^\circ$ .



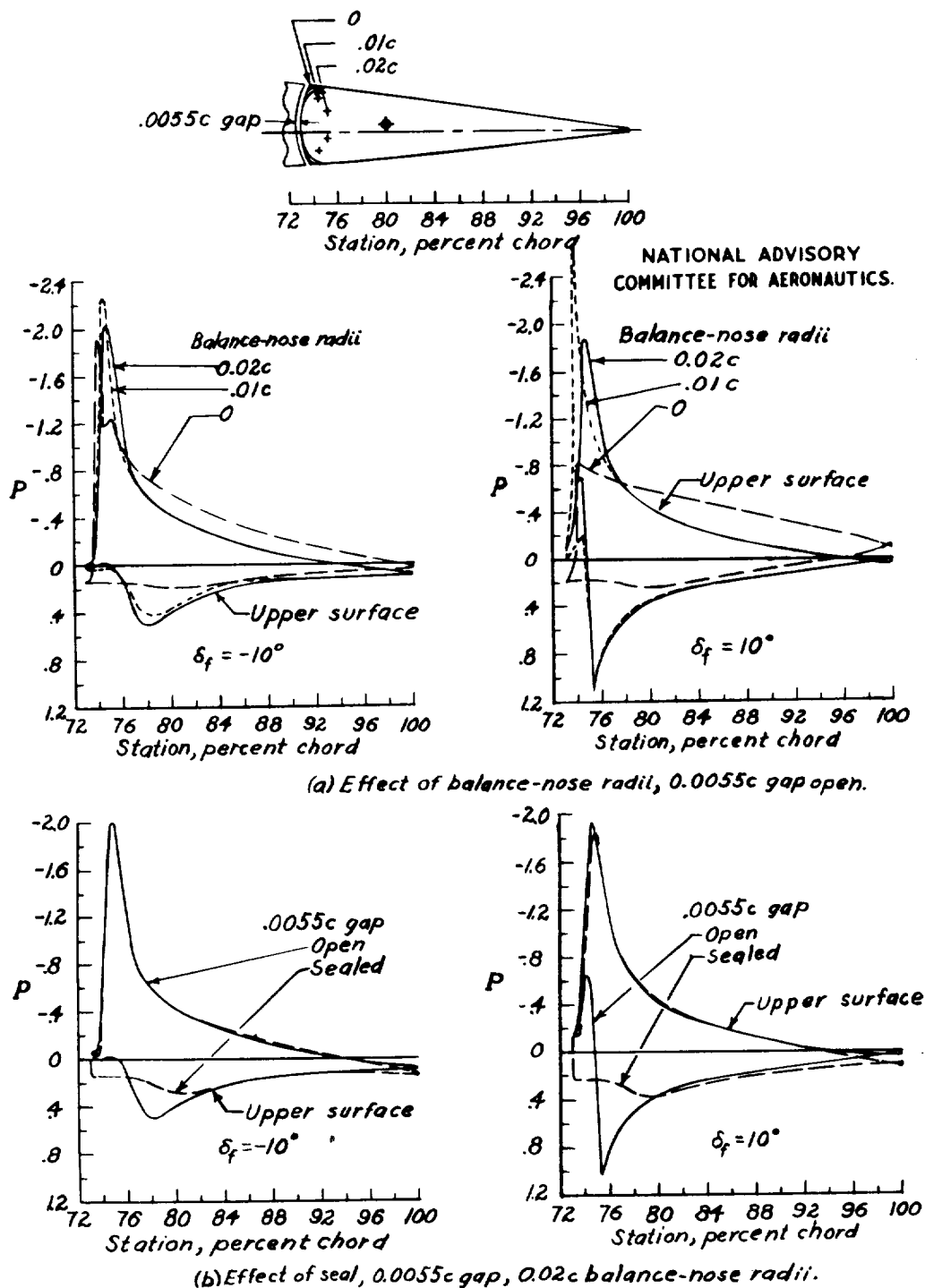


Figure 9.- Pressure distributions on a  $0.20c$  flap with a  $0.35c_f$  blunt-nose balance. NACA 23012 airfoil section (model I of table II); data from reference 26;  $\alpha, 0^\circ$ ;  $M \approx 0.36$ .





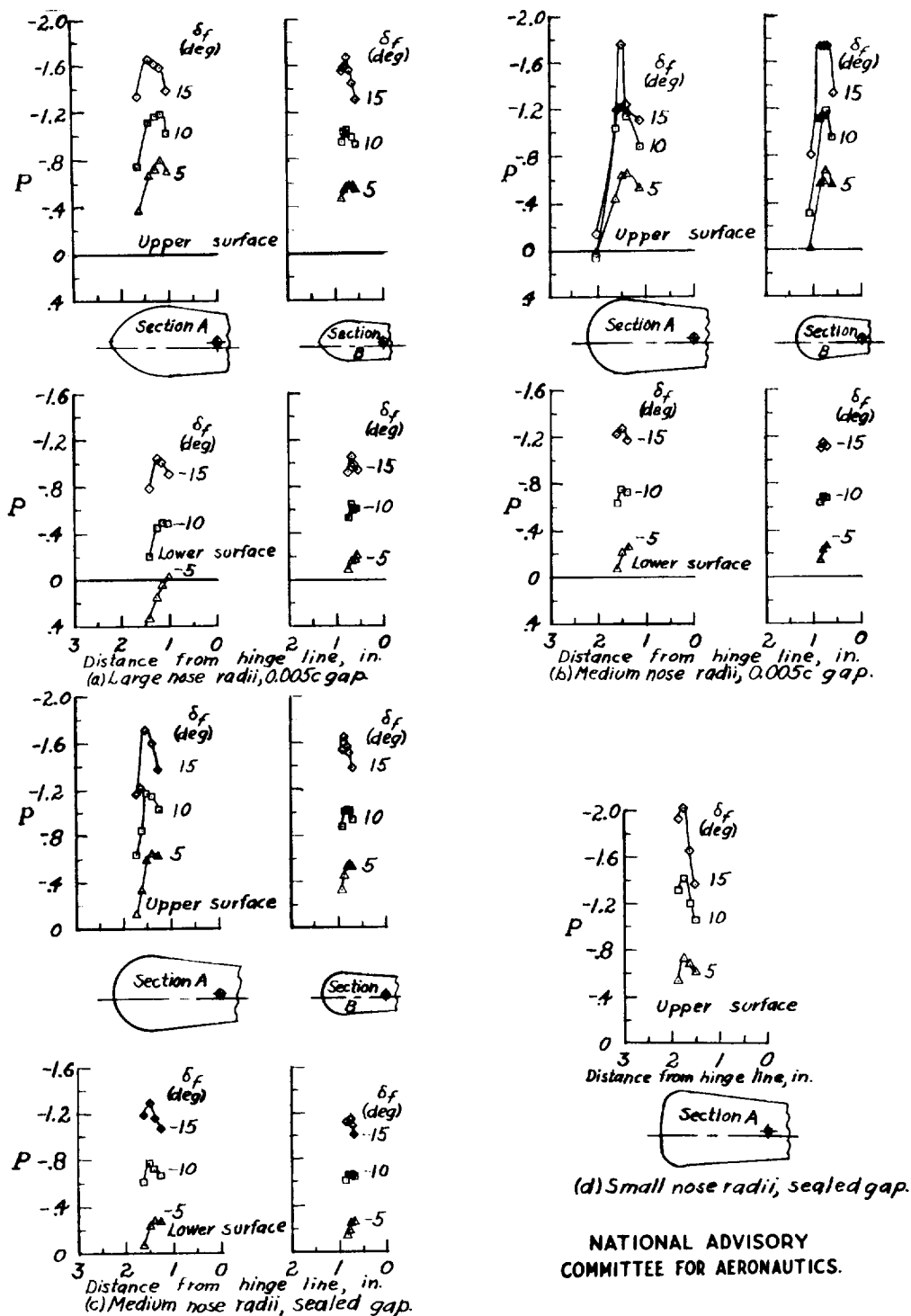


Figure 10.- Effect of aileron deflection and nose shape on the peak pressures at the nose of a 0.155c aileron with a 0.35 $c_f$  balance. Model IX of table II; data from reference 19;  $\alpha$ , 0°;  $M \approx 0.1$ .



L-665

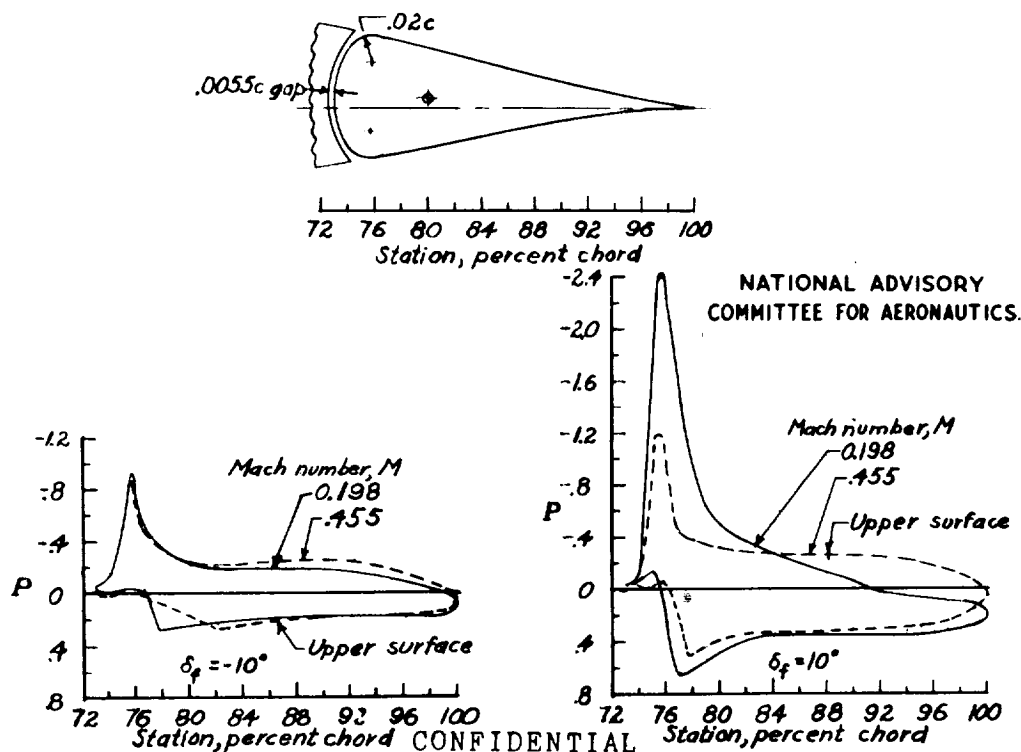


Figure 11.- Pressure distributions on a  $0.20c$  flap with a  $0.35c_f$  blunt-nose balance. NACA 66(215)-216,  $\alpha = 1.0$  airfoil section; model II of table II; data from reference 26;  $\alpha, 0^\circ$ ; gap,  $0.0055c$ .

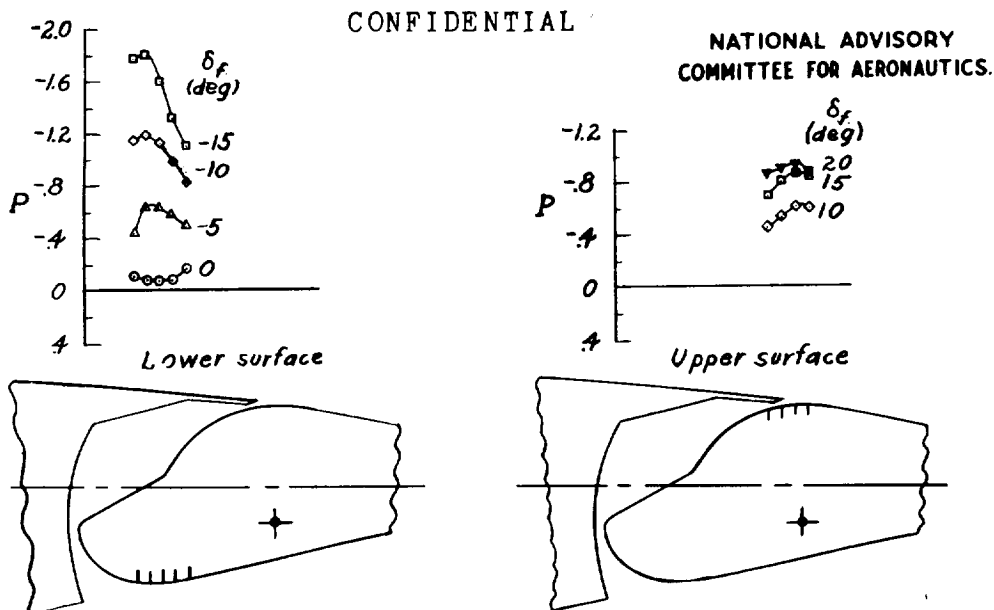


Figure 12.- Effect of aileron deflection on peak pressures of a  $0.20c$  aileron with a  $0.40c_f$  Frise balance. Model XIX of table II. Data from reference 1;  $\alpha, 1^\circ$ ;  $M \approx 0.1$ .



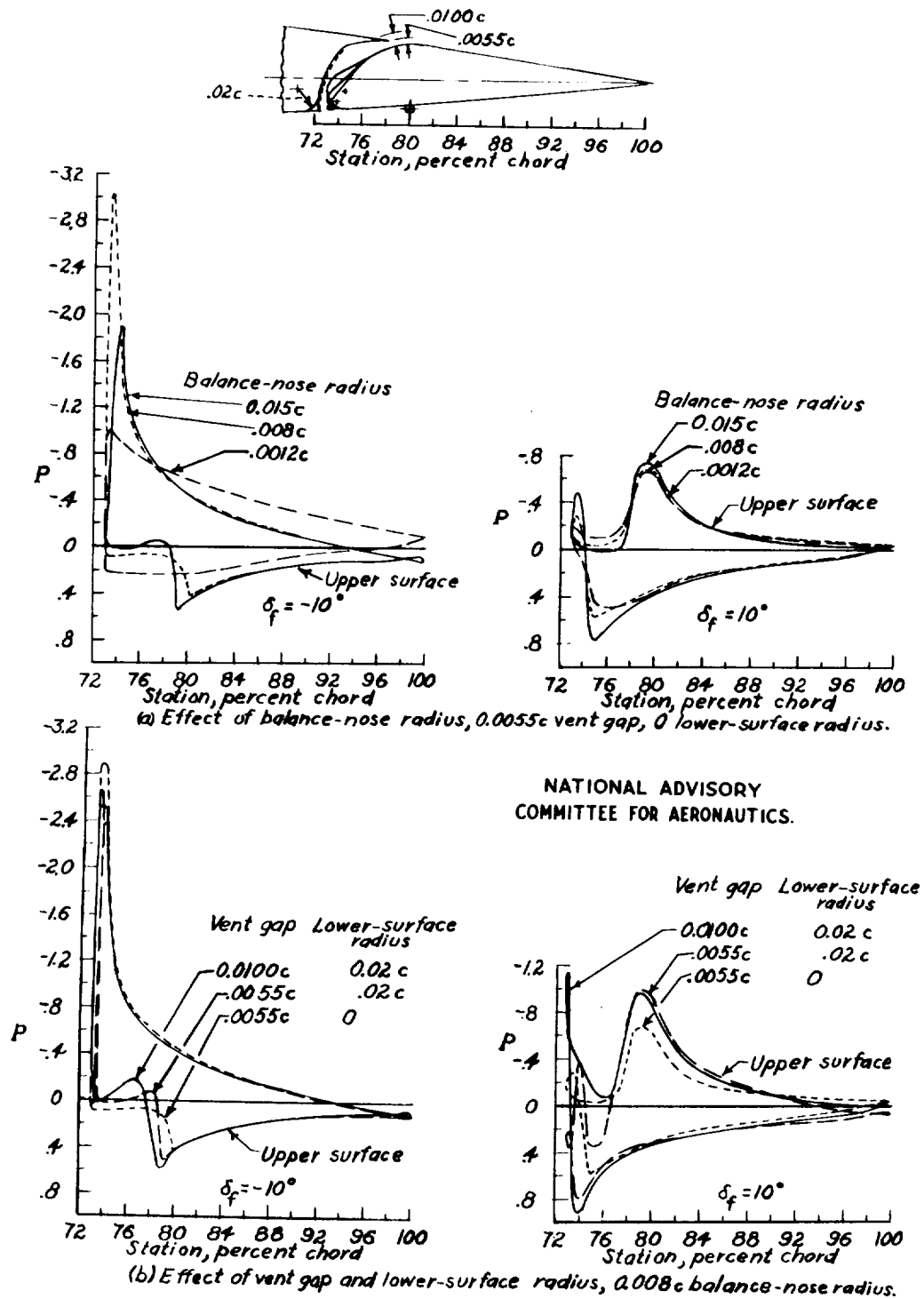
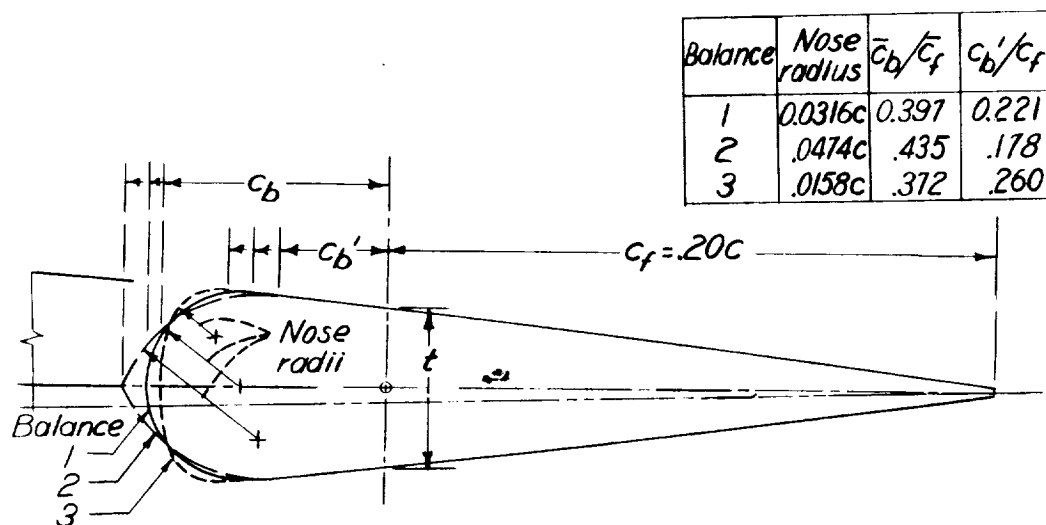


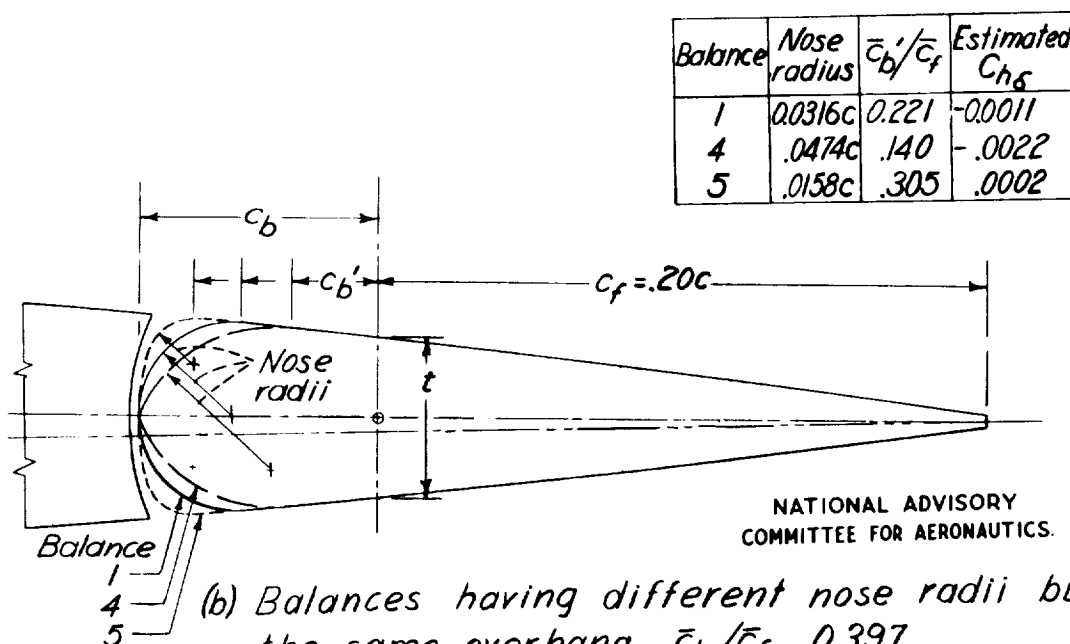
Figure 13.- Pressure distributions on a  $0.20c$  flap with a  $0.35c_f$  Frise balance. NACA 23012 airfoil section; model XVI of table II; data from reference 26;  $\alpha, 0^\circ$ ;  $M, 0.36$ .



L-665



(a) Balances having different nose radii and different overhangs but the same balance factor.  $K_1$ , 0.074;  $\frac{\bar{t}/2}{\bar{c}_f}$ , 0.131; estimated  $C_{h\delta}$ , -0.0011.



NATIONAL ADVISORY  
COMMITTEE FOR AERONAUTICS.

(b) Balances having different nose radii but the same overhang.  $\bar{c}_b/\bar{c}_f$ , 0.397.

Figure 14.- Various plain-overhang balances derived for ailerons of wing used for illustrative example. NACA 23012 airfoil;  $\bar{c}_f/\bar{c}$ , 0.20;  $\frac{\bar{t}/2}{\bar{c}_f}$ , 0.131;  $\bar{c}_b/\bar{c}_f$ , 0.397.

